

Lawrence Berkeley National Laboratory

LBL Publications

Title

Evaluation of hydrograph separation techniques with uncertain end-member composition

Permalink

<https://escholarship.org/uc/item/2zw8f9zm>

Journal

Hydrological Processes, 36(9)

ISSN

0885-6087

Authors

Lukens, Eileen

Neilson, Bethany T

Williams, Kenneth H

et al.

Publication Date

2022-09-01

DOI

10.1002/hyp.14693

Copyright Information

This work is made available under the terms of a Creative Commons Attribution-NonCommercial License, available at <https://creativecommons.org/licenses/by-nc/4.0/>

Peer reviewed

1 Evaluation of Hydrograph Separation Techniques with Uncertain End- 2 member Composition

3 **Running Head:** Evaluating Hydrograph Separation Techniques

4
5 E. Lukens¹, B.T. Neilson¹, K.H. Williams^{2,4}, J. Brahney³

6 ¹Utah Water Research Laboratory, Department of Civil and Environmental Engineering, Utah
7 State University, 8200 Old Main Hill, Logan, UT, 84322, United States

8 ²Earth and Environmental Sciences, Lawrence Berkeley National Laboratory, Berkeley, CA,
9 94720, United States

10 ³Department of Watershed Sciences, Utah State University, 5210 Old Main Hill, Logan, UT,
11 84322, United States

12 ⁴Rocky Mountain Biological Laboratory, Gothic, CO, 81224, United States

13
14 **Corresponding Author:** Janice Brahney, Department of Watershed Sciences, Utah State
15 University, 5210 Old Main Hill, Logan, UT, 84322, United States.

16 Email: (Janice.Brahney@usu.edu)

17 18 **Abstract**

19 Hydrograph separation is one of many approaches used to analyze shifts in source water
20 contributions to stream flow resulting from climate change in remote watersheds. Understanding
21 these shifts is vital, as shifts in source water contributions to a stream can shape water
22 management decisions. Because remote watersheds are often inaccessible and have poorly
23 characterized contributing water sources, or end-members, it is critical to understand the
24 implications of using different hydrograph separation techniques in these data-limited
25 environments. To explore the uncertainty associated with different techniques, results from two
26 hydrograph separation techniques, mass balance and principle component analysis, were
27 compared using three years of aqueous geochemical data from the East River watershed located
28 in the Elk Mountains of Central Colorado. Solute concentrations of the end-members were
29 characterized by both a limited set of direct chemical measurements of different sources and
30 detailed seasonal instream chemistry to examine the influences of uncertain end-member
31 compositions in a data-limited environment. Annual volumetric end-member contributions to
32 stream flow had relatively good agreement across separation techniques. Large variations in time
33 were observed in the hydrograph separations, depending on the end-member type, and estimated
34 flow contributions varied between the selected solutes. End-member concentrations
35 characterized by stream chemistry showed several limitations including a reduced number of
36 distinguishable end-members and differences in timing of flow contributions. Results highlight
37 the benefits of using multiple hydrograph separation techniques by providing a ‘weight-of-
38 evidence’ approach to environments with limited end-member concentration data.

39
40 **Keywords:** hydrograph separation, mass balance, end-member mixing, instream chemistry, data-
41 limited, solutes

42 **1. INTRODUCTION**

43 The hydrology of high-elevation mountain environments has changed dramatically over
44 the past decade (Hock et al., 2019). April 1st snow water equivalent, an important hydrologic
45 indicator, has been in decline across the western United States in part due to rising global
46 temperatures (Mote et al., 2005; Mote et al., 2018; Huning & AghaKouchak, 2018) and an
47 increase in the fraction of precipitation falling as rain (Hamlet et al., 2005; Knowles et al., 2006).
48 This is significant as a decrease in the fraction of precipitation falling as snow has been identified
49 as one cause of decreased streamflow (Berghuijs et al., 2014; Foster et al., 2016), along with
50 shifts in evaporative losses (Foster et al., 2016). Additionally, the timing of snow derived runoff
51 has been observed to occur earlier than long term averages across western North America
52 (Brahney et al., 2017a; Clow, 2010; Stewart et al., 2005), which has been exacerbated by dust
53 deposition on snow (Painter et al., 2007; Skiles et al., 2012). Earlier snowmelt may cause high
54 elevation reservoirs to exceed storage capacities, forcing early releases (Barnett et al., 2005 &
55 references therein; Kopytkovskiy et al., 2015). This loss of storage as snow and storage within
56 reservoirs means less water during periods of summer drought when water demand is high. This
57 is consequential as agriculture is particularly vulnerable to shifts in snowmelt quantity in the
58 western United States (Qin et al., 2020), where 53% of annual runoff is snow derived (Li et al.,
59 2017). This is even higher in mountainous regions where 70% of annual runoff is snow derived
60 (Li et al., 2017). Changes to the timing, duration, and quantity of snowmelt may also impact
61 sensitive endemic instream biota (Brahney et al., 2020; Brown et al., 2007) and may affect the
62 biodiversity of cold water adapted organisms (Hotaling et al., 2017 & references therein). Given
63 that shifts in source water contributions to instream flow are influential in the genetic diversity
64 and management of mountain stream systems, techniques to track these changes in remote
65 environments are critical.

66 Hydrograph separation techniques are often used to separate the chemically distinct
67 source waters (end-members) contributing to instream flow. Traditionally, hydrograph
68 separations are performed using mass balances with one or two chemical or isotopic solutes (see
69 Klaus & McDonnell, 2013; Wels et al., 1991). Another more robust form of hydrograph
70 separation additionally utilizes principal component analysis (PCA) and end-member mixing
71 analysis (EMMA). This second method offers an advantage by employing a larger suite of
72 chemical and isotopic information than a traditional mass balance to separate the end-members

73 (see Bearup et al., 2014; Carroll et al., 2018; Liu et al., 2017). This partitioning of flow into the
74 end-members through hydrograph separation techniques is useful for analyzing changes in the
75 hydrology of mountain catchments. For example, hydrograph separation has been used to track
76 temporal changes in glacial contributions to streamflow (Brahney et al., 2017b), analyze base
77 flow patterns in the Upper Colorado River Basin (Miller et al., 2014), and examine how forest
78 bark beetle infestations affect the local water balance (Bearup et al., 2014). Studies such as these
79 demonstrate the power and versatility of hydrograph separation techniques. Using multiple
80 separation techniques offers both a method of comparison and also a potential ‘weight-of-
81 evidence’ approach to working in catchments where a single separation technique on its own
82 may not fully characterize the contributing end-members.

83 Components that contribute to instream flow can generally be categorized into “old” (pre-
84 event) and “new” (event) waters, as summarized by Genereux & Hooper (1998). Old water is
85 usually described as all water that exists in the watershed before hydrologic perturbation, such as
86 a rainstorm or snowmelt event that generally reaches the stream through subsurface pathways.
87 New water may reach the stream by infiltrating and taking short residence time subsurface
88 pathways or may enter the stream through surface pathways (Freeze, 1974). Residence time in
89 the watershed is an important factor as it will affect the chemical signal a packet of water
90 accumulates as it moves towards the stream. Sueker et al., (2000) summarizes this well,
91 describing water that undergoes significant chemical changes as ‘reacted’ water and water that
92 goes unaltered through the watershed as ‘unreacted’ water. Thus, instream chemistry represents
93 the complex mix of source waters existing as new and old water and having undergone (or not
94 undergone) a chemical alteration. To parse the contribution of these unique water types to
95 streams, hydrograph separations can be used in tandem with geochemically relevant solute
96 information from the stream and the contributing end-members. For accurate separations, solute
97 concentrations of the contributing end-members should be representative of the end-members
98 throughout the basin. However, detailed spatial and temporal information about end-member
99 solute concentrations are very difficult to establish. As highlighted by Bales et al. (2006),
100 spatially detailed hydrologic observation networks in mountainous environments are often
101 unavailable.

102 As such, data limitations often affect the number of possible end-members that are
103 identified and how end-member concentrations are characterized. Studies often choose to

104 approach characterizing end-member concentrations one of two ways. Some studies (Jenkins et
105 al., 1994; Liu et al., 2017; Williams et al., 2009) characterize end-member concentrations
106 through detailed temporal and spatial sampling directly from the sources. The second way is
107 through a type of ‘hydrologic rationalization’ in which end-member concentrations are
108 characterized solely by instream data during certain flows or at certain locations (Pinder & Jones,
109 1969, Miller et al. 2014, and Foks et al., 2019). For example, the stream's chemical composition
110 during periods of low flow is often assigned to a groundwater end-member. Still, other studies
111 use a combination of detailed sampling and hydrologic rationalization to characterize end-
112 member concentrations. For example, James & Roulet (2009) utilized diverse spatial sampling to
113 characterize a concentration range for a new-water end-member. Detailed instream sampling
114 during baseflow along with samples from a single spring in the study area were used to
115 characterize concentrations of an old-water end-member. Many studies have highlighted the
116 issues with using poorly characterized end-member concentrations to perform hydrograph
117 separations (Cayuela et al., 2019; Kiewiet et al., 2020; Penna & Meerveld, 2019), but
118 characterizing end-member concentrations via detailed spatial and temporal sampling is not
119 always possible, particularly in remote catchments. This highlights the need to develop methods
120 to overcome inevitable end-member data limitations.

121 Understanding the strengths and weaknesses of different hydrograph separation
122 techniques in predicting end-member contributions when end-member information is limited is a
123 critical first step. Therefore, this study focuses on *how two similar hydrograph separation*
124 *techniques compare in their prediction of annual volumetric end-member contributions to rivers*
125 *with limited end-member data, but detailed instream data across multiple years*. Of specific
126 interest are 1) the consequences of using different end-member characterizations informed by
127 detailed instream data to address challenges related to spatially limited end-member data with
128 two commonly applied hydrograph separation techniques and 2) if any general conclusions about
129 catchment hydrology can be made as a result of using multiple separation techniques and a
130 ‘weight-of-evidence’ approach.

131

132 **2. METHODS**

133 **2.1 Study Area**

134 The experimental watershed is located in the Gunnison National Forest near Gothic,
135 Colorado (Figure 1) and serves as the primary drainage of the main stem East River (ER). The
136 study site includes the Rocky Mountain Biological Laboratory (RMBL) and hosts a diversity of
137 hydrogeochemical studies performed as part of the Lawrence Berkeley National Laboratory
138 (LBNL) Watershed Function Science Focus Area (WFSFA) funded by the U.S. Department of
139 Energy. The headwaters of the ER are in a high-alpine region of the Elk Mountains of Central
140 Colorado at an elevation of 3190 m, and with the confluence of the Taylor River near Almont,
141 Colorado form the Gunnison River at an elevation of 2245 m. The sub-watershed of interest has
142 a drainage area of approximately 85 km². The ER represents one of the many small watersheds
143 that drain to the Upper Colorado River Basin (UCRB), a critical water resource for much of the
144 western United States. The ER WFSFA receives 1200 mm yr⁻¹ of precipitation (PRISM, 2021)
145 that primarily falls as snow (Hubbard et al. 2018). The ER watershed is generally considered
146 pristine and runoff is composed primarily of snowmelt, rain, and groundwater (Carroll et al.,
147 2018) with little to no human impact in the study area apart from atmospheric deposition events.
148 The arid regions of the southwestern United States have been identified as a likely source of dust
149 deposition in the Colorado Rockies (Lawrence et al. 2010). Dust in the Colorado Rocky
150 Mountains is commonly calcareous (Brahney et al., 2013; Clow et al., 2016) and has been
151 observed to shift snowmelt by one to three weeks earlier than pre-dust loading conditions (Clow
152 et al. 2016; Painter et al., 2010; Skiles et al. 2015). The geology of the area is dominated by
153 Mancos shale of Cretaceous age with intrusions of Paleogene igneous laccoliths and ore-rich
154 stocks (Hubbard et al. 2018). For additional information about the study site, see Hubbard et al.
155 (2018).

156

157 [Insert Figure 1]

158

159 **2.2 Data Collection**

160 **2.2.1 Instream Sampling**

161 Associated with ongoing research as part of the WFSFA, LBNL investigators have been
162 collecting stream discharge and solute data at daily to weekly intervals beginning in May 2014 at
163 one instream monitoring site located at the watershed outlet (Pumphouse (PH), Figure 1). The
164 PH site is located at an elevation of 2760 m and includes an automated water sampler (Model

165 3700; Teledyne ISCO, NE, USA) to recover stream water samples from a fixed location in the
166 stream channel via a peristaltic pump into uncapped 1 L polyethylene bottles. Geochemical
167 analysis of all water samples includes cations, trace metals, and anions. Prior to analysis, samples
168 were filtered (Pall, NY, USA; polytetrafluoroethylene: 0.45 μ m) and stored at 4 C. Anion samples
169 were stored in high-density polyethylene vials with Cl, NO₃, and SO₄ measured using an ion
170 chromatograph (ICS-2100, Dionex, CA, USA) equipped with AS-18 analytical and guard
171 columns with concentrations determined using factory-provided calibration standards. Cation
172 samples were preserved with trace metal grade 12N HNO₃ and analyzed using ion coupled
173 plasma mass spectrometry (Element 2, Thermo Fisher, MA, USA). For this study, only solutes
174 from the 2016, 2017, and 2018 water years (WYs) were used (where the 2016 WY is defined as
175 October 1st, 2015 to September 30th, 2016). The PH site also includes a multi-parameter sonde
176 (EXO2; YSI, Inc.; Yellow Springs, OH, USA) equipped with an EXO conductivity/temperature
177 sensor for measuring the specific conductivity (SC) of stream water at 5-minute intervals over
178 the WY2016-2018 interval.

179 ***2.2.2 End-member sampling***

180 Two potential end-members were sampled (snow and deep groundwater). Snow samples
181 were collected from 2017 to 2020 with the majority of samples collected in 2020 at six locations
182 around the basin (Snow pits, Figure 1). Snow pits were dug in open, flat areas with anion, cation,
183 and trace metal concentrations determined by filtering (Pall, NY, USA; polytetrafluoroethylene:
184 0.45 μ m) melted samples collected at 10 cm intervals over the pit depth. Pit depths ranged from
185 67 to 140.5 cm depending upon location. Solute data representative of deep (~60 m) groundwater
186 sourced from Mancos shale bedrock has been monitored weekly to monthly since 2015 at the
187 Inouye Well, which is drilled to a depth of 61 m with water pumped to the ground surface from
188 this depth using a fixed downhole pump. Samples were filtered upon collection and stored at 4
189 °C until analysis. For this study, only groundwater samples collected in the 2016 – 2018 WYs
190 were used.

191

192 **2.3 Hydrograph Separation Approaches**

193 Two methods of hydrograph separation and two characterization methods for end-
194 member concentrations were used to compare volumetric contributions to instream flow using
195 limited end-member data, but detailed instream chemistry data for three water years (WYs). The

196 first hydrograph separation technique used PCA and EMMA. PCA is a statistical tool that uses
197 the variances and co-variances of datasets to highlight collective trends. The purpose of this type
198 of analysis is to identify a shared factor (such as an end-member) that may explain trends
199 exhibited in a mixing space. EMMA employs a statistical analysis of the mixing space to identify
200 end-members based on instream chemical signals (Christophersen & Hooper 1992). However,
201 this method is fundamentally reliant on mass balance principles and since the mixing space
202 consists of projected solute concentration data, it can be used in tandem with flow data in a
203 constrained system of equations to solve for the contributions to instream flow due to each end-
204 member. This approach of using PCA and EMMA for hydrograph separation is herein referred to
205 as the ‘statistically-based approach’ although it utilizes mass balance principles for the final step
206 of the hydrograph separation. Several important assumptions are made to ensure the validity of
207 this approach. First, EMMA requires the assumption of the conservative (linear) mixing of end-
208 members (Christophersen et al., 1990; Christophersen & Hooper, 1992). In addition, EMMA
209 requires end-members to have a constant composition or the variability in end-member
210 composition must be known through time and/or space. The last requirement is that end-member
211 concentrations must be sufficiently different from each other for at least one solute
212 (Christophersen et al., 1990; Hooper et al., 1990).

213 The second method of hydrograph separation used was a simple chemical mass balance.
214 Chemical data are collected to characterize the composition of each source water. These data,
215 along with instream concentration and discharge data, are then used in a constrained system of
216 equations where mass is conserved to parse the contribution of each source water (Pinder &
217 Jones, 1969). This approach is herein referred to as the ‘mass-based’ approach. Several
218 assumptions are applied that are similar to those established by Sklash & Farvolden (1979) and
219 those from the statistically-based method of separation. These include: 1) that end-member
220 composition is assumed constant or else the variability in time and/or space is known, 2) solutes
221 mix conservatively, 3) the number of end-members are known, 4) instream concentrations are
222 only composed of waters originating from the identified end-members or else all other waters
223 contributing are considered negligible, and 5) end-member concentrations are sufficiently
224 different for at least one solute.

225 End-member concentrations were characterized using two methods because of the
226 uncertainties associated with limited end-member measurements. The first characterization of the

227 end-member concentrations was by direct sampling of two potential end-members (groundwater
228 and snowmelt) at a limited number of sites across the basin (Figure 1). The second method of
229 characterizing end-member concentrations was done by inferring potential end-members from
230 instream chemistry during certain flow regimes at certain times of the year at the outlet of the
231 catchment. Hereinafter, end-member concentrations characterized by direct sampling of the
232 source waters will be referred to as ‘measured end-member concentrations’ and end-member
233 concentrations characterized by instream sampling at the outlet of the catchment during certain
234 flows and times of the year will be referred to as ‘hydrologically rationalized end-member
235 concentrations’. These two characterizations of the concentrations of the end-members have
236 unique ranges and both of these will be discussed in further detail in the following sections.

237 By using these two hydrograph separation techniques and two different characterizations
238 of the end-members, five types of separations were performed for the 2016, 2017, and 2018 WYs
239 (Figure 2). Each separation offers insight into the possible separation of the hydrograph and the
240 associated variability.

241

242 [Insert Figure 2]

243

244 ***2.3.1 Solute Selection***

245 The solutes used in both methods play an essential role in determining the outcome of the
246 hydrograph separation. Different combinations of solutes will yield slightly different answers.
247 Non-conservative solutes or solutes without geochemical relevance to the basin will result in
248 poor separations. Four different methods were used to select the solutes for both analyses. First,
249 commonly used conservative solutes in hydrograph separations were examined. Second,
250 conservative solutes used previously at this specific study site were examined. Third, the
251 temporal behavior of instream solutes was examined. Fourth, solute behavior in relation to flow
252 was examined. In the statistically-based approach, a posteriori method can also be used to select
253 solutes. This posteriori method involves plotting measured instream concentrations against
254 predicted instream solute concentrations, resulting from end-member concentrations and
255 fractional flow contributions informed by the statistically-based hydrograph separation. If
256 predictions are sufficient, as evaluated by coefficients of determination and slopes, the solutes
257 can be retained in the analysis. If not, new solutes can be selected.

258 Commonly used conservative solutes in hydrograph separation methods include calcium,
259 magnesium, potassium, silicon, and sodium, as was shown by Wels et al. (1991), Hooper (2003),
260 and Liu et al. (2017). Less commonly used solutes include rubidium, barium, strontium,
261 uranium, and (sometimes) sulfate as shown in Ladouche et al. (2001) and Barthold et al. (2011).
262 A previous study done in ER WFSFA used calcium, uranium, strontium, sulfate, and two stable
263 isotopes to perform their separation in the 2016 WY; but, they suggested that sulfate not be used
264 in future studies in the basin due to observed non-conservative behavior (Carroll et al., 2018).

265 Time series of solute data were also analyzed (Figures S1-S3). This was helpful for
266 identifying solutes with clear temporal patterns (e.g., Ca or Na) and those without clear temporal
267 patterns (e.g., Sn or V). After examining temporal behaviors, the solute's relation to flow was
268 used as the final *a priori* metric of selection for solutes to be used in the analysis (see, Ladouche
269 et al., 2001; Pinder & Jones, 1969). Examining the temporal behavior of solutes is important as it
270 can change from year to year. The linearity of solute concentrations in this study was quantified
271 and classified based on hydrologic responsiveness to changes in flow. High coefficients of
272 determination (R^2), slope, and low root mean square error (RMSE) produced from the
273 comparison of a linear best-fit on logarithmic concentration – discharge (C-Q) plots were used as
274 indicators for the strength of the relationship (Table 1) (Godsey et al., 2009). If solutes qualified
275 as “Best” or “Moderate” in two of the three categories, they were retained for use in the analysis
276 for that WY (Table S1). This was done to find solutes that mobilize with changes in runoff
277 generation and to highlight seasonal end-members. It is important to note that linearity in C-Q
278 plots indicates conservative mixing, likely between just two end-members; however, it is
279 possible there could be more if two end-members had similar solute concentrations. Because this
280 method of selecting solutes is also highly effective at highlighting solutes that are responsive to
281 changes in end-member contributions that influence instream concentrations, it was used in
282 tandem with the other three methods described previously.

283

284 [Insert Table 1]

285

286 **2.3.2 End-member Characterization**

287 **2.3.2.1 Hydrologically Rationalized End-member Concentrations**

288 Using our general understanding of hydrology in this area, three potential end-members
289 (deep groundwater, snowmelt, and soil water) were identified and then characterized from the
290 detailed instream solute data at the outlet of the catchment. These hydrologically rationalized
291 end-member concentration ranges were chosen to capture the chemical variability instream over
292 time. This characterization of end-member concentration ranges may be helpful indicators of
293 changes in end-member contributions to the stream throughout the year when detailed end-
294 member concentration data are limited or unavailable.

295 Commonly, deep groundwater concentrations are inferred from instream chemistry
296 during base flow (see James & Roulet, 2009; Miller et al., 2014, Pinder & Jones 1969). As such,
297 solute concentrations during the lowest 5% of discharge were used to represent deep
298 groundwater chemistry. Similarly, solute concentrations during the highest 5% of discharge were
299 used to represent snowmelt when deep groundwater contributions are limited and snowmelt
300 dominates runoff in mountainous systems such as the UCRB. While this characterization of the
301 snowmelt end-member concentrations will not perfectly represent the variability in snow
302 composition, it does provide a reasonable representation of the variability in the integrated snow
303 end-member contributions to instream chemistry. Finally, shallow soil waters were characterized
304 by using the highest 15% of discharge from the summer storm events in August through October.
305 This period was chosen as any deviation in base flow chemistry late in the water year that was
306 likely due to storm events and could represent older and reacted water. It is important to note that
307 characterizing end-member concentrations based on instream chemistry will bias hydrograph
308 separation results to 100% contribution of the defined end-member during the respective flow
309 regimes. To account for variability in the hydrologically rationalized end-member
310 concentrations, a normal distribution was assumed using the mean and standard deviation of each
311 end-member. This distribution was randomly sampled 1000 times to establish a range of possible
312 source compositions for each solute to be used in the hydrograph separations.

313 *2.3.2.2 Measured End-member Concentrations*

314 The second method of characterizing end-member concentrations used measured values.
315 To establish measured end-member concentration ranges for each solute representing two
316 potential end-members (snowmelt and deep groundwater), we created distributions based on a
317 limited number of available solute samples. This provided insight into acceptable concentration
318 ranges for the two measured and potential end-members. The snowmelt sample size was small (n

319 = 18 – 36) and represented six sample sites from the basin from 2017 to 2020. Because of the
320 small sample size, we established a uniform distribution based on the min and max of the field
321 samples and randomly sampled it 1000 times to get at the possible source concentrations for each
322 solute (Figures S4 – S8). This was done to better represent the uncertainty in the measured end-
323 member concentration for each solute to be used in hydrograph separations.

324 The number of measured groundwater samples was spatially limited. The field samples
325 collected from 2016 WY through the 2018 WY (n =122-124) from a single location, the Inouye
326 Well, were nearly normally distributed (Figures S9 – S13). A distribution was generated for each
327 solute based on the distribution inherent to the field samples collected by LBNL and sampled
328 1000 times to determine possible groundwater compositions. The resulting concentrations from
329 each sampled distribution were then used in the hydrograph separation techniques.

330 As with hydrologically rationalized end-member concentrations, characterizing end-
331 member concentrations via direct measurements also poses challenges. Acquiring representative
332 source samples can be difficult in mountain environments where there may be significant spatial
333 variation. In addition, end-member concentrations can change significantly while en route to the
334 stream. This is why creating distributions from our limited set of measured data was important to
335 represent uncertainty in end-member composition.

336

337 **2.3.3 PCA and EMMA**

338 To begin the statistically-based method of hydrograph separation, first the PCA must be
339 performed. Through PCA, stream chemistry is projected into a mixing space (referred to as the
340 *U*-space) defined by the principal components retained for analysis (Equations S1-S3).
341 Determining the number of principal components to retain is significant as the number of end-
342 members is one greater than the number of principal components retained. To do this, \mathbf{X} – which
343 represents the standardized matrix containing time series of stream chemistry - is projected into
344 the *U*-space while maintaining the units in the solute space (*S*-space) following (Christophersen
345 & Hooper, 1992; Equation 1)

$$\hat{\mathbf{X}} = \mathbf{X}\mathbf{V}'(\mathbf{V}\mathbf{V}')^{-1}\mathbf{V} \quad (1)$$

346 where $\hat{\mathbf{X}}$ is the de-standardized but projected matrix of \mathbf{X} that has units equivalent to that of the
347 *S*-space, and \mathbf{V} is the eigenvector obtained from the PCA. The residuals (Hooper, 2003; Equation

348 2) between the modeled stream chemistry in the projected matrix and the measured stream
349 chemistry are calculated as

$$E_j = \widehat{X}_j - X_j \quad (2)$$

350 where E is the matrix of residuals between the projected j th solutes and the measured j th solutes.
351 Generally, if the modeled data is a good fit to the observed data, the residuals should be identical
352 and normally distributed with a mean of zero and constant variance (Draper & Smith, 1981). If
353 the residuals violate any of these conditions, it suggests that there is a pattern within the data that
354 the model is not capturing. As such, residuals were analyzed using the coefficient of
355 determination (R^2) and relative root mean square error (RRMSE) to evaluate structure and
356 variance. Residuals were also analyzed using p -values to find significant ($p < 0.05$) linear trends
357 in the residuals and analyzed with quantile-quantile plots to evaluate normality. RRMSE
358 (Equation 3) was calculated as

$$RRMSE = \frac{\sqrt{\frac{\sum E_j^2}{n}}}{\overline{X}_j} \quad (3)$$

359 where \overline{X}_j represents the average solute concentration and n represents the number of samples.
360 Similar studies have also used R^2 and/or RRMSE (e.g. Ali et al., 2010; Bearup et al., 2014;
361 Carroll et al., 2018) to quantify the residuals (Table S2). These studies were used as a basis for
362 comparison to determine appropriately low R^2 and RRMSE values. Using these metrics, the
363 number of principal components (m) as well as the predicted number of end-members were
364 determined. To complete the analysis, all solutes and end-members were projected into the U -
365 space (Equations S4 & S5).

366

367 **2.4 Hydrograph Separation**

368 **2.4.1 Statistical Hydrograph Separation**

369 The final steps of the statistically-based approach result in a set of linear equations, which
370 can then be solved using the constrained least-squares method. A constrained least-squares
371 method was used in order to accommodate end-member concentrations characterized by
372 hydrologic rationalization. To separate the hydrograph, the system of equations (Equation 4) is
373 solved for f , the fraction of instream signal due to each end-member. An example of the system

374 of equations in the instance of three end-members is shown below; but, it can be easily reduced
 375 in the instance that only two end-members are found to describe the mixing space.

$$\begin{cases} 1 = f_1 + f_2 + f_3 \\ \mathbf{U}_1 = \mathbf{W}_1^1 f_1 + \mathbf{W}_1^2 f_2 + \mathbf{W}_1^3 f_3 \\ \mathbf{U}_2 = \mathbf{W}_2^1 f_1 + \mathbf{W}_2^2 f_2 + \mathbf{W}_2^3 f_3 \end{cases} \quad (4)$$

where f due to each end – member ≥ 0

376 \mathbf{W} is known and represents the projected end-member in the U -space, with subscripts
 377 indicating the principal component and superscripts indicating the identity of the end-member.
 378 \mathbf{U} represents the projected solutes instream with the subscripts again indicating the
 379 corresponding principal component. In instances of just two end-members, the system of
 380 equations was reduced accordingly. \mathbf{W} was selected from the end-member distributions
 381 described previously to solve the system of equations. This was done 1000 times to produce
 382 1000 different solutions to Equation 1. For each iteration, the end-member fraction was
 383 multiplied by the stream flow to calculate the flow due to that end-member. This resulted in a
 384 1000 possible separated hydrograph solutions for each time-step to reflect the variability in
 385 potential end-member concentrations.

386

387 **2.4.2 Mass Balance Separation**

388 For mass balance separations, the number of end-members and the identity of the end-
 389 members are decided *a priori*. Since the ER is a snow-dominated basin in the UCRB, deep
 390 groundwater and snowmelt were two logical and likely choices for end-members, but they were
 391 assumed end-members. A third end-member was not included in this method of separation, but
 392 could be in future studies. To separate the hydrograph using a mass balance, discharge and
 393 concentration data were combined in a system of just two equations. The first equation in the
 394 system below represents a flow balance where unaltered groundwater and snow water are
 395 assumed to mix instantaneously in the water column. This equation (Equation 5) represents a
 396 mass balance with a particular solute.

$$\begin{cases} Q_{tot} = Q_{gw} + Q_{sm} \\ C_{tot} Q_{tot} = C_{gw} Q_{gw} + C_{sm} Q_{sm} \end{cases} \quad (5)$$

397 Q_{tot} is the total instream discharge measured at the Pumphouse, Q_{gw} and Q_{sm} and represent
 398 discharges from groundwater and snowmelt. C_{tot} is the concentration instream at the

399 Pumphouse. C_{gw} and C_{sm} are the measured concentrations at the groundwater and snow end-
400 members, respectively. Like the statistical separation, C_{gw} and C_{sm} were selected from the
401 generated distributions described previously for both measured and hydrologically rationalized
402 end-members. The system of equations was solved 1000 times for Q_{gw} and Q_{sm} for each time
403 step to generate 1000 possible hydrograph separations.

404

405 **3. RESULTS**

406 **3.1 Solute Selection**

407 The C-Q plots revealed that the solutes with the strongest relationship to discharge were
408 generally calcium, uranium, and strontium for all years analyzed (Table S1; Figures S14 -S16).
409 Solute were often inversely correlated with discharge (Figures S17 – S19). Barium strongly
410 correlated to discharge in both the 2016 and 2018 WYs, and as a result, it was also used in the
411 2017 WY. Given that strontium met all criteria sufficiently in 2016 WY and 2018 WY, it was
412 also used in 2017 WY despite only meeting one out of the two criteria for retention defined in
413 Table 1. Magnesium correlated strongly with discharge in the 2016 WY and was included for
414 that water year only. Sulfate, a commonly used solute in mixing analyses, albeit one that is not
415 conservative, had a strong correlation to discharge. Previous research by Carroll et al. (2018)
416 suggested it may not be conservative in this watershed owing to anaerobic forms of microbial
417 reduction, and therefore, it was subsequently excluded from this analysis. In summary, the
418 selected solutes used in all years were barium, calcium, strontium, and uranium, with magnesium
419 used only in the 2016 WY.

420

421 **3.2 End-members**

422 ***3.2.1 End-member Concentration Distributions***

423 The individual end-member solute concentration distributions that were sampled for
424 hydrograph separation differed based on the method of characterization (hydrologically
425 rationalized or measured). For end-member concentrations characterized by hydrologic
426 rationalization, solute concentrations were randomly sampled from the generated normal
427 distributions described previously. For end-member concentrations characterized by field
428 measurements, solute concentrations were sampled from generated uniform distributions for the
429 snow end-member (Figures S4-S8). Solute concentrations for the groundwater end-member were

430 sampled from the generated distributions inherent to the field samples of groundwater (Figures
431 S9-S13).

432

433 **3.2.2 End-member Retention**

434 Following an analysis of the residuals and principal component space, the number of end-
435 members contributing to instream flow was determined. For all water years, the residuals as
436 evaluated by R^2 and RRMSE indicated the retention of two to three principal components (Table
437 2). The number of end-members is one more than the number of principal components; hence,
438 three to four end-members were predicted. Although R^2 and RRMSE values are reasonable based
439 on accepted ranges in similar studies (Table S2), none of the residuals were normally distributed
440 according to the quantile-quantile plots (Figures S20 – S31). This indicates that there could be
441 aspects of mixing space that are not entirely captured by the solutes included in the analysis.
442 Results from the residuals as evaluated by p-values are variable, but generally agree that four
443 end-members could adequately describe the mixing space. P-values often (although not always)
444 indicated slopes significantly ($p < 0.05$) different than zero for $m \leq 2$, which suggests some
445 remaining pattern in the residuals at low levels of principal component retention. An example of
446 these results for the 2016 WY are shown below for strontium (Figure 3). Overall, R^2 and
447 RRMSE indicated that the calculated principal components adequately described the mixing
448 space for the purposes of this study, but quantile-quantile plots and p-values results vary and
449 suggest that this analysis could be improved in the future, such as by testing different solute
450 combinations in an aim to reduce structure in residuals.

451

452 [Insert Table 2]

453

454 [Insert Figure 3]

455

456 For all water years, similar trends in the projections of solutes into the mixing space (U -
457 space) were observed (Figure 4). Projection into the U -space indicates that solutes have seasonal
458 variation. The stream signal tends towards the snow end-member during peak runoff and then
459 towards the groundwater end-member during periods of base flow. The collective non-linear
460 shape of the projected solutes in the U -space support the findings from the residuals analysis and

461 suggests the existence of more end-members than identified. Thus, based on the collective
462 information from all analyses, three major end-members are likely. Given the ER WFSFA is a
463 snow-dominated basin with seasonal melt, it was assumed that groundwater and snow water
464 were two likely contributors to the stream. The possibility of a potential third major end-member
465 (soil water) was tested using hydrologically rationalized end-member concentrations with the
466 statistically-based method of hydrograph separation. However, this was not possible in
467 separations with measured end-member concentrations due to limited end-member data. Since
468 groundwater and snow are assumed, it is possible that they are not the primary streamflow
469 controls, rather they are likely contributors based on previous work done in the ER basin by
470 Carroll et al., (2018). In summary, instream flow was assumed to be composed of water
471 originating from two to three end-members, with three end-members being most likely. The
472 implications of potential missing end-members in hydrograph separations done with only two
473 end-members are discussed in more detail in the following sections.

474

475 [Insert Figure 4]

476

477 **3.3 Hydrograph Separations**

478 With the solutes and the number of end-members selected, hydrograph separations
479 proceeded. Recall the hydrographs were separated using two different methods with two
480 different end-member characterizations (Figure 2). In addition, both two and three end-member
481 separations were tested.

482

483 ***3.3.1 Statistically-based Hydrograph Separation***

484 *3.3.1.1 Three End-members Characterized by Hydrologic Rationalization (3 H-EM)*

485 Using hydrologically rationalized end-member concentrations, a separation was
486 performed to yield a groundwater component, a snow water component, and a soil water
487 component (Figure 5). Error bands show the interquartile ranges (IQR) resulting from the
488 sampling of the end-member distributions. The initial flush of groundwater generally peaks in
489 May while the snow signal tends to peak in June, with this behavior being generally replicable
490 across water years. In contrast, soil water contributions vary across years. Increases in soil water
491 contributions during June may be related to precipitation events (Figure S32), but direct

492 causation is unclear. Large variations seen in the 2017 WY may be due to the inclusion of
493 barium even though it lacked a strong relationship with discharge in the 2017 WY. A feature to
494 note in all separations done with hydrologically rationalized end-member concentrations is the
495 short period of time in June where there is no evident contribution of groundwater. This is an
496 artifact of using hydrologically rationalized end-members and will be discussed in detail in the
497 following sections.

498

499 *3.3.1.2 Two End-members Characterized by Hydrologic Rationalization (2 H-EM)*

500 Using two end-members with hydrologically rationalized concentrations, the hydrograph
501 was separated into a groundwater and a snow water component (Figure S33). While the
502 discharge contribution of each end-member differs slightly from that of a three end-member
503 separation, the timing of the peak groundwater contribution is the same. Similar to the separation
504 with three end-members, there is again an artifact from the methodology where groundwater
505 contributions in all water years go to zero for one to two weeks in June.

506

507 [Insert Figure 5]

508

509 *3.3.1.3 Two End-members Characterized by Measurements (2 M-EM)*

510 Using two end-members characterized by measured concentrations rather than the
511 hydrologically rationalized concentrations, there is a difference in the timing of peak
512 groundwater contributions (Figure 6). In this separation, where two measured end-member
513 concentrations are used, groundwater peaks with peak snowmelt rather than before peak
514 snowmelt. This difference in timing is likely due to the two different characterizations of the
515 end-members. In addition, discharge contributions from snow are greater than groundwater
516 contributions at most times of the year. This occurs even when there is no snow in the basin (e.g.,
517 during the late summer and early winter months). However, a potential missing soil water end-
518 member may help to explain this discrepancy as soil water can enter the stream during these
519 times.

520

521 *3.3.1.4 Model Evaluation*

522 As stated previously, selected solutes were examined posteriori by comparing predicted
523 versus measured instream concentrations in the statistically-based method. In general, predicted
524 versus measured instream concentrations showed strong relationships across all years as
525 indicated by high R^2 values (Figures S34 – S40). However, separations with measured end-
526 member concentrations showed consistent underestimations of instream concentrations of
527 calcium and barium, and consistent over estimations of strontium (Figures S34 - S35). This is
528 demonstrated well in the 2016 WY (Figure 7). Uranium was well predicted with measured end-
529 member concentrations. Instream concentrations of solutes were well predicted with models
530 using hydrologically rationalized end-member concentrations, which was expected as the
531 hydrologically rationalized end-member concentrations were derived from the stream chemistry
532 (Figure 8; Figures S6 – S40). In general, residuals indicate that most solutes were able to predict
533 instream concentrations reasonably well (as seen by the relatively normal distribution of the
534 residuals) with the exception of barium in the 2017 WY; however, end-member concentrations
535 characterized by measurements generally over or under predicted instream concentrations in
536 some capacity. This suggests that the model could be improved in future studies by testing
537 different solutes and solute combinations in an effort to estimate instream concentrations more
538 consistently (Barthold et al., 2011).

539

540 [Insert Figure 6]

541

542 [Insert Figure 7]

543

544 [Insert Figure 8]

545

546 **3.3.2 Mass-based Hydrograph Separation**

547 *3.3.2.1 Two End-members Characterized by Hydrologic Rationalization (2 H-EM)*

548 Using two end-members with hydrologically rationalized concentrations in a mass
549 balance separation yielded similar results as the statistically-based method of separation (Figure
550 9). Again, the timing of peak groundwater contribution is shifted so that it occurs before peak
551 snowmelt, which is an artifact of using hydrologically rationalized end-member concentrations.
552 However, the mass balance method reveals how the separation is affected by different solutes

553 (Figure S41). There is a clear separation of the hydrograph in all water years and good agreement
554 among all solutes with the exception of barium in 2017 WY (Figure S41).

555

556 3.3.2.2 *Two End-members Characterized by Measurements (2 M-EM)*

557 Similar to a statistical separation of the hydrograph using two end-members based on
558 field measurements, the mass-based separation method also showed groundwater and snowmelt
559 peaking at the same time. When the median response of all solutes is assessed, the IQR is quite
560 large (Figure S42). However, using the mass-based method, the influence of each solute can be
561 examined (Figures S43). Viewing solutes individually, it is clear that calcium is very different
562 from the other solutes, predicting an almost 50/50 split in the flow contributions of each end-
563 member during the entire water year. When calcium is removed from the analysis (Figure S44),
564 the IQR is greatly decreased and there is a better separation of groundwater and snow water
565 contributions (Figure 10). Again, barium is a poor solute for separation the 2017 WY.

566

567 [Insert Figure 9]

568

569 [Insert Figure 10]

570

571 **3.4 End-member Fractions of Total Annual Volumes**

572 Since there are several differences in the time series of the separated hydrographs due to
573 the different methods and end-member characterizations, annual volumetric contributions of end-
574 members to stream flow were used as another method of comparison (Figure 11, Table 3).

575 Across methods, the median percent of total annual volume from groundwater ranged from 21%
576 to 41% from 2016 - 2018 (regardless of the number of end-members or the characterization of
577 the end-members). Median annual groundwater contributions from hydrologically rationalized
578 end-member concentrations ranged from 21% – 41%, while median groundwater contributions
579 estimated from measured end-member concentrations had a slightly smaller range from 22% –
580 35%. In general, the IQR of the same end-member number and characterization overlap
581 regardless of the method of hydrograph separation. Overall, these results suggest that the median
582 percent annual volumes of the end-members are similar across hydrograph separation techniques

583 and vary more across end-member characterization. However, there are large variations in the
584 mass-based method of separation depending on the solute used (Figure S45).

585

586 [Insert Table 3]

587

588 [Insert Figure 11]

589

590 **4. DISCUSSION**

591 Hydrograph separations via statistically-based and mass-based methods with two unique
592 end-member characterizations were used to analyze the hydrology of a catchment with limited
593 end-member data but detailed instream data. Results highlight the importance of solute choice as
594 well as end-member retention and characterization in separations. In addition, annual volumes
595 were similar despite differences in timing caused by different end-member characterizations.

596

597 **4.1 Selected Solutes**

598 Selected solutes influenced results in both statistical and mass-based methods of
599 separation. Although solutes were selected using multiple methods, selection procedures were
600 heavily reliant on the solute's hydrologic responsiveness to flow, which generally assumes
601 simple mixing of two end-members. In addition, choosing solutes that changed with flow
602 prioritized solutes that mobilized strongly (as opposed to periodically or weakly) with flow. In a
603 detailed end-member mixing study by Barthold et al. (2011), it was found that geochemically
604 similar elements like magnesium and calcium (both of which mobilize fairly well with
605 discharge) could potentially deliver similar information and suggested it may be better to include
606 more minor elements. Thus, our analysis may be flawed in that minor elements that did not
607 mobilize with flow were not included, even though they may have offered a broader perspective
608 of basin hydrology.

609 Limiting the number of solutes could also unintentionally exclude important
610 hydrogeochemical indicators in the watershed. This is well demonstrated by mass-based
611 separation results wherein two solutes stand out as behaving very differently from the others.
612 The first is calcium in separations with measured end-member concentrations, which often
613 predicts a 50/50 contribution of end-members at all times of the year across all water years

614 (Figure S43). As a result, when examining the median response from all solutes, including
615 calcium (Figure S42), there is a much larger total IQR than without calcium (Figure 10).
616 Interestingly, in contrast to the analysis with measured end-member concentrations, a mass-
617 based separation with hydrologically rationalized end-member concentrations has a very clear
618 separation using calcium (Figure S41). This variation across end-member characterization is very
619 different from other solutes, such as strontium and uranium, that produce clear separations
620 regardless of being derived from measured or hydrologically rationalized end-member
621 concentrations. Barium also tends to act like strontium and uranium in all years except in the
622 2017 WY. In this year, barium tends to dramatically and rapidly change end-member response
623 (Figures S41 and S44). Barium shows the significant temporal variations a solute can have in a
624 catchment from year to year and it may not have behaved conservatively or been appropriate to
625 include in the analysis for 2017 WY.

626 Although the barium's 2017 WY behavior may be partly due to its weak relationship with
627 discharge in this year (Table S1), it also illustrates the utility of more solutes or different
628 combinations of solute in providing additional information. Perhaps other minor elements would
629 behave similarly and prompt investigation into the presence of additional unidentified end-
630 members (e.g., ephemeral springs or creeks sporadically discharging to the river after storm
631 periods). Alternatively, the use of additional solutes could highlight non-conservative behaviors
632 or other reactive processes occurring via different hydrologic flows paths. Non-conservative
633 behavior is a critical consideration while examining the separated hydrograph as it could affect
634 the amount of water attributed to an end-member during the water year. Beyond considering the
635 selection of solutes, testing multiple combinations of solutes within PCA is one advantage of the
636 statistically-based method that was not included here. Testing additional solute combinations in
637 the future may allow for better estimates of instream solute concentrations for solutes such as
638 calcium, which was consistently underestimated using measured end-member concentrations
639 (Figure 7; S34 - S35). All in all, the behaviors demonstrated by individual solutes stress the
640 importance of choosing appropriate solutes that can capture the full basin hydrology, particularly
641 in environments where sampling is limited. A broader range of conservative solutes based on
642 multiple catchment characteristics (hydrology, geology, atmospheric deposition patterns, etc.)
643 may prove to be beneficial. Future studies will need to explore the solute selection process more

644 deeply and perhaps establish additional methods that can guide researchers to the
645 hydrogeochemically pertinent solutes for their catchment.

646

647 **4.2 Implications of End-member Characterization and Retention**

648 **4.2.1 End-member Characterization**

649 In this study, end-member data was limited. Besides direct end-member measurements,
650 hydrologic rationalization of end-members based on instream chemistry was used to characterize
651 end-member concentrations. Using these two end-member characterization methods led to
652 several substantial differences in the resulting separated hydrographs.

653

654 *4.2.1.1 Hydrologically Rationalized End-member Concentrations*

655 Figures 5 and 9 display two features that are unique to hydrograph separations done with
656 hydrologically rationalized end-member concentrations. The first is a difference in the timing of
657 peak groundwater contributions to earlier in the year than separations performed with measured
658 end-member concentrations. This is because hydrologically rationalized end-member
659 concentrations are close in magnitude to (or at times, the same as) the instream concentrations.
660 This similarity to instream concentrations makes it so small chemical shifts in the stream can
661 indicate more dramatic shifts in end-member contributions, hence the earlier increase in peak
662 groundwater contribution to the stream as compared to separations performed with measured
663 end-member concentrations. Subsequently, the difference between instream concentrations and
664 measured end-member concentrations is much larger, so small changes in the instream
665 concentration of solutes indicate small changes in end-member contributions. Hence, only when
666 there are substantial changes in the composition of the stream are dramatic shifts in the
667 contributing end-members indicated.

668 The other important feature of hydrograph separations done with hydrologically
669 rationalized end-members is the period of zero contribution of groundwater during peak
670 snowmelt. The reason for this is well demonstrated by the principal component mixing space
671 (Figure 4). It is clear that hydrologically rationalized end-member concentrations can overlap
672 with the instream solutes allowing 100% contribution of that end-member to instream flow at a
673 given time of year (Figures 5 & S41). This is a violation of the end-member mixing model
674 assumptions that state end-members must be a convex combination that encompass the solutes in

675 the mixing space (Christophersen & Hooper, 1992; Hooper, 2003; Hooper et al., 1990).
676 Furthermore, the mixing space can be encompassed by any number of end-members, but with
677 hydrologically rationalized end-member concentrations it is very hard to distinguish more than
678 three contributing end-members that can encompass the solutes in the mixing space.

679 Despite this, hydrologically rationalized end-member concentrations may pose an
680 advantage in data-limited environments. Hydrologically rationalized end-member concentrations
681 – unlike measured end-member concentrations - do not require spatially and temporally uniform
682 end-member data or detailed sampling schemes. Rather, hydrologically rationalized end-member
683 concentrations derived from instream data are able to provide a snapshot of the major end-
684 member contributors to streamflow during the year. Hence in studies where distinctions between
685 more than three end-members are not needed, hydrologically rationalized end-members may
686 offer unique and desirable benefits such as the reduced sample location requirements (just
687 needing one at the outlet of the catchment).

688

689 *4.2.1.2 Measured End-member Concentrations*

690 Some measured end-member concentration data was available for use in the hydrograph
691 separations. This was important, as it gave evidence for the observed solute concentration ranges
692 of the possible end-members. Ideally, the measured composition of an end-member for a
693 hydrograph separation should be representative of the end-member composition for the entire
694 watershed. In this study, a single sampling point at the Inouye Well was used to represent all
695 groundwater regardless of depth or bedrock composition. However, a USGS geologic survey of
696 the area shows a diverse geologic profile (Gaskill et al., 1991) that suggests such spatially
697 limited sampling of the groundwater end-member likely insufficiently captured the range of
698 possible groundwater concentrations within the 85 km² basin. Other studies have also noted
699 spatial (Penna & Meerveld, 2019) and temporal (Feng et al., 2002; Liu et al., 2004) variability in
700 end-member composition. Furthermore, the spatial and temporal variability in end-member
701 composition and its effect on the hydrograph has been observed in catchments < 1 km² in size
702 (Cayuela et al., 2019; Kiewiet et al., 2020). Studies such as these emphasize the importance of
703 spatially diverse and temporally detailed end-member data for hydrograph separation. However,
704 this is not always possible in remote catchments with limited access, financial, and/or personnel

705 resources and highlights how multiple methods of separation may be useful when detailed end-
706 member data is limited or unavailable.

707

708 **4.2.2 End-member Retention**

709 With limited end-member data available, this study included two possible end-members
710 with concentrations characterized by field measurements (groundwater and snowmelt) and three
711 possible end-members with concentrations characterized by hydrologic rationalization
712 (groundwater, snowmelt, and soil water). However, residuals and *U*-space analysis indicated that
713 three to four end-members would best capture basin hydrology (Tables S3 – S5; Figure 4). As
714 such, there is likely an over attribution of flow to the end-members that were available for use in
715 the separations. For example, in separations where just two end-members characterized by
716 measured concentrations are present, snowmelt contributions are predicted even when no
717 snow was present in the basin like during the late summer (after July) and early fall months
718 (Figures 6 and 10). This over attribution of flow to the snow end-member may have been due to
719 missing end-members in the analysis, such as soil water or rainfall producing overland flow.

720

721 **4.3 Annual Volumetric End-member Contributions**

722 Across hydrograph separation methods, total percent of annual volume from each end-
723 member was generally similar with median groundwater contributions ranging between 21% and
724 41% (Table 3; Figure 11). These findings agree reasonably well with other studies of the UCRB.
725 Miller et al. (2014) performed a solute separation across multiple sub-basins in the UCRB
726 finding that annual contributions of base flow to discharge ranged between 21 and 58% in large
727 basins (>1000 km²). This estimate is expected to be greater as the study areas are much larger.
728 However, there was a study conducted previously in a sub-basin of the ER WFSFA where a
729 hydrologic water budget revealed groundwater contributions ranged from 21 to 52% with an
730 average of 35% (Carroll et al., 2019). Our findings using a limited set of end-member data
731 appears relatively consistent with the much more data-detailed study Carroll et al., (2019) in the
732 same watershed; although, there is variation based on the characterization of the end-member
733 concentrations and the solutes used in the analysis. Overall, these findings seem to suggest that
734 in the face of limited data, multiple methods of hydrograph separation may be useful in tracking
735 shifts in the hydrology of mountainous and seasonally snow-dominated catchments.

736

737 **5. CONCLUSIONS**

738 Using limited end-member data and multiple conservative solutes, two hydrograph
739 separation techniques were compared. Results showed that there can be large temporal
740 differences in the predicted hydrograph based on the characterization of end-members and
741 solutes used. Consequences of characterizing end-member concentrations through hydrologic
742 rationalization include reduced numbers of distinguishable end-members, shifts in the timing of
743 end-member contributions to the stream, and periods of time where some end-member
744 contributions go to 100% and others become zero. However, the benefits of using hydrologically
745 rationalized end-member concentrations include the requirement of a single sampling point
746 which could be advantageous in data-limited environments so long as their limitations are
747 appropriately considered within the context of individual catchments. Results additionally show
748 that annual volumetric contribution of the end-members to instream flow were similar across
749 hydrograph separation techniques and provided reasonable annual volumetric estimates of the
750 groundwater end-member. However, estimates of annual volumetric contributions of the end-
751 members do vary depending on the characterization of end-member concentrations (measured or
752 hydrologically rationalized). The results suggest that in remote mountainous catchments where
753 data is limited, the use of multiple hydrograph separation techniques could provide valuable
754 information about shifting water resources. This is critical considering the growing significance
755 of water coming from remote catchments and the role such water plays in the security and
756 management of our water future and sensitive mountain ecosystems.

757

758 **ACKNOWLEDGEMENTS**

759 Thank you to all the contributors and collaborators who made this study possible. All
760 data used in this paper were collected, analyzed, and made available by the Lawrence Berkeley
761 National Laboratory. This work was funded by the Utah Water Research Laboratory and the U.S.
762 Department of Energy (DOE) award DE-FOA-0001724. This material is partially based upon
763 work supported through the Lawrence Berkeley National Laboratory's Watershed Function
764 Science Focus Area. The DOE, Office of Science, Office of Biological and Environmental
765 Research funded the work under contract DE-AC02-05CH11231 (Lawrence Berkeley National
766 Laboratory; operated by the University of California). This work was additionally supported by

767 the U.S. National Science Foundation under grant numbers 2043363, 2044051, and 2043150. We
768 would also like to thank the four anonymous reviewers who provided comments and suggestions
769 for resubmission, as well as Caleb Buahin who also provided feedback.

770

771 **DATA AVAILABILITY**

772 All data used in the analysis are available through the Lawrence Berkley National Laboratory at
773 <https://data.ess-dive.lbl.gov/view/doi:10.21952/WTR/1495380> and [https://data.ess-](https://data.ess-dive.lbl.gov/view/doi:10.15485/1668055)
774 [dive.lbl.gov/view/doi:10.15485/1668055](https://data.ess-dive.lbl.gov/view/doi:10.15485/1668055). Snow pit data from the Lawrence Berkley National
775 Laboratory will be made available soon at <https://data.ess-dive.lbl.gov/>, along with a data
776 package specific to this publication.

777 **REFERENCES**

- 778 Ali, G. A., Roy, A. G., Turmel, M.-C., & Courchesne, F. (2010). Source-to-stream connectivity
779 assessment through end-member mixing analysis. *Journal of Hydrology*, 392(3), 119–135.
780 <https://doi.org/10.1016/j.jhydrol.2010.07.049>
- 781 Bales, R.C., Molotch, N.P., Painter, T.H., Dettinger, M. D., Rice, R., & Dozier, J. (2006).
782 Mountain Hydrology of the western United States, *Water Resources Research*, 42(8),
783 <https://doi.org/10.1029/2005WR004387>
- 784 Barnett, T. P., Adam, J. C., & Lettenmaier, D. P. (2005). Potential impacts of a warming climate
785 on water availability in snow-dominated regions. *Nature*, 438(7066), 303–309.
786 <https://doi.org/10.1038/nature04141>
- 787 Barthold, F. K., Tyralla, C., Schneider, K., Vaché, K. B., Frede, H.-G., & Breuer, L. (2011).
788 How many tracers do we need for end member mixing analysis (EMMA)? A sensitivity
789 analysis. *Water Resources Research*, 47(8). <https://doi.org/10.1029/2011WR010604>
- 790 Bearup, L. A., Maxwell, R. M., Clow, D. W., & McCray, J. E. (2014). Hydrological effects of
791 forest transpiration loss in bark beetle-impacted watersheds. *Nature Climate Change*, 4(6),
792 481–486. <https://doi.org/10.1038/nclimate2198>
- 793 Berghuijs, W. R., Woods, R. A., & Hrachowitz, M. (2014). A precipitation shift from snow
794 towards rain leads to a decrease in streamflow. *Nature Climate Change*, 4(7), 583–586.
795 <https://doi.org/10.1038/nclimate2246>
- 796 Brahney, J., Ballantyne, A. P., Sievers, C., & Neff, J. C. (2013). Increasing Ca²⁺ deposition in
797 the western US: The role of mineral aerosols. *Aeolian Research*, 10, 77–87.
798 <https://doi.org/10.1016/j.aeolia.2013.04.003>
- 799 Brahney, J., Bothwell, M. L., Capito, L., Gray, C. A., Null, S. E., Menounos, B., & Curtis, P. J.
800 (2020). Glacier recession alters stream water quality characteristics facilitating bloom
801 formation in the benthic diatom *Didymosphenia geminata*. *Science of The Total*
802 *Environment*, 142856. <https://doi.org/10.1016/j.scitotenv.2020.142856>
- 803 Brahney, J., Menounos, B., Wei, X., & Curtis, P. J. (2017b). Determining annual cryosphere
804 storage contributions to streamflow using historical hydrometric records. *Hydrological*
805 *Processes*, 31(8), 1590–1601. <https://doi.org/10.1002/hyp.11128>
- 806 Brahney, J., Weber, F., Foord, V., Janmaat, J., & Curtis, P. J. (2017a). Evidence for a climate-
807 driven hydrologic regime shift in the Canadian Columbia Basin. *Canadian Water*
808 *Resources Journal / Revue Canadienne Des Ressources Hydriques*, 42(2), 179–192.
809 <https://doi.org/10.1080/07011784.2016.1268933>
- 810 Brown, L. E., Hannah, D. M., & Milner, A. M. (2007). Vulnerability of alpine stream
811 biodiversity to shrinking glaciers and snowpacks. *Global Change Biology*, 13(5), 958–
812 966. <https://doi.org/10.1111/j.1365-2486.2007.01341.x>
- 813 Carroll, R. W. H., Bearup, L. A., Brown, W., Dong, W., Bill, M., & Williams, K. H. (2018).
814 Factors controlling seasonal groundwater and solute flux from snow-dominated basins.
815 *Hydrological Processes*, 32(14), 2187–2202. <https://doi.org/10.1002/hyp.13151>
- 816 Carroll, R. W. H., Deems, J. S., Niswonger, R., Schumer, R., & Williams, K. H. (2019). The
817 Importance of Interflow to Groundwater Recharge in a Snowmelt-Dominated Headwater
818 Basin. *Geophysical Research Letters*, 46(11), 5899–5908.
819 <https://doi.org/10.1029/2019GL082447>
- 820 Cayuela, C., Latron, J., Geris, J., & Llorens, P. (2019). Spatio-temporal variability of the isotopic
821 input signal in a partly forested catchment: Implications for hydrograph separation.
822 *Hydrological Processes*, 33(1), 36–46. <https://doi.org/10.1002/hyp.13309>

- 823 Christophersen, N., & Hooper, R. P. (1992). Multivariate analysis of stream water chemical data:
 824 The use of principal components analysis for the end-member mixing problem. *Water*
 825 *Resources Research*, 28(1), 99–107. <https://doi.org/10.1029/91WR02518>
- 826 Christophersen, N., Neal, C., Hooper, R. P., Vogt, R. D., & Andersen, S. (1990). Modelling
 827 streamwater chemistry as a mixture of soilwater end-members—A step towards second-
 828 generation acidification models. *Journal of Hydrology*, 116(1), 307–320.
 829 [https://doi.org/10.1016/0022-1694\(90\)90130-P](https://doi.org/10.1016/0022-1694(90)90130-P)
- 830 Clow, D. W. (2010). Changes in the timing of snowmelt and streamflow in Colorado: A response
 831 to recent warming. *Journal of Climate*, 23(9), 2293–2306. USGS Publications Warehouse.
 832 <https://doi.org/10.1175/2009JCLI2951.1>
- 833 Clow, D. W., Williams, M. W., & Schuster, P. F. (2016). Increasing aeolian dust deposition to
 834 snowpacks in the Rocky Mountains inferred from snowpack, wet deposition, and aerosol
 835 chemistry. *Atmospheric Environment*, 146, 183–194.
 836 <https://doi.org/10.1016/j.atmosenv.2016.06.076>
- 837 Davis, J. (2002). *Statistics and Data Analysis in Geology* (3rd ed.). John Wiley & Sons, INC.
- 838 Draper, N. R., & Smith, H. (1981). *Applied Regression Analysis* (2nd ed.). John Wiley & Sons,
 839 INC.
- 840 Feng, X., Taylor, S., Renshaw, C. E., & Kirchner, J. W. (2002). Isotopic evolution of snowmelt
 841 1. A physically based one-dimensional model. *Water Resources Research*, 38(10), 35-1-
 842 35–38. <https://doi.org/10.1029/2001WR000814>
- 843 Foks, S. S., Raffensperger, J. P., Penn, C. A., & Driscoll, J. M. (2019). Estimation of Base Flow
 844 by Optimal Hydrograph Separation for the Conterminous United States and Implications
 845 for National-Extent Hydrologic Models. *Water*, 11(8), 1629.
 846 <https://doi.org/10.3390/w11081629>
- 847 Foster, L. M., Bearup, L. A., Molotch, N. P., Brooks, P. D., & Maxwell, R. M. (2016). Energy
 848 budget increases reduce mean streamflow more than snow–rain transitions: Using
 849 integrated modeling to isolate climate change impacts on Rocky Mountain hydrology.
 850 *Environmental Research Letters*, 11(4), 044015. <https://doi.org/10.1088/1748-9326/11/4/044015>
- 851 Freeze, R.A. (1974). Streamflow generation, *Rev. Geophys. and Space Physics*, 12(4), 627-647.
- 852 Gaskill, D. L., Mutschler, F. E., Kramer, J. H., Thomas, J. A., & Zahony, S. G. (1991). *Geologic*
 853 *Map of the Gothic quadrangle (GQ-1689)* [Map]. USGS.
 854 https://ngmdb.usgs.gov/Prodesc/proddesc_1199.htm
- 855 Genereux, D., & Hooper, R. (1998). *Chapter 10 – Oxygen and Hydrogen Isotopes in Rainfall-Runoff Studies*. <https://doi.org/10.1016/B978-0-444-81546-0.50017-3>
- 856 Godsey, S. E., Kirchner, J. W., & Clow, D. W. (2009). Concentration–discharge relationships
 857 reflect chemostatic characteristics of US catchments. *Hydrological Processes*, 23(13),
 858 1844–1864. <https://doi.org/10.1002/hyp.7315>
- 859 Hamlet, A. F., Mote, P. W., Clark, M. P., & Lettenmaier, D. P. (2005). Effects of Temperature
 860 and Precipitation Variability on Snowpack Trends in the Western United States. *Journal*
 861 *of Climate*, 18(21), 4545–4561. <https://doi.org/10.1175/JCLI3538.1>
- 862 Hock, R., Rasul, C., Adler, C., Cáceres, B., Gruber, S., Hirabayashi, Y., Jackson, M., Kääb, A.,
 863 Kang, S., Kutuzov, S., Milner, A., Molau, U., Morin, S., Orlove, B., & Steltzer, H. (2019).
 864 *High Mountain Areas*. In: *IPCC Special Report on the Ocean and Cryosphere in a*
 865 *Changing Climate*. IPCC. <https://www.ipcc.ch/srocc/chapter/chapter-2/>

868 Hooper, R. P. (2003). Diagnostic tools for mixing models of stream water chemistry. *Water*
869 *Resources Research*, 39(3). <https://doi.org/10.1029/2002WR001528>

870 Hooper, R. P., Christophersen, N., & Peters, N. E. (1990). Modelling streamwater chemistry as a
871 mixture of soilwater end-members—An application to the Panola Mountain catchment,
872 Georgia, U.S.A. *Journal of Hydrology*, 116(1), 321–343. [https://doi.org/10.1016/0022-](https://doi.org/10.1016/0022-1694(90)90131-G)
873 1694(90)90131-G

874 Hotaling, S., Hood, E., & Hamilton, T. L. (2017). Microbial ecology of mountain glacier
875 ecosystems: Biodiversity, ecological connections and implications of a warming climate.
876 *Environmental Microbiology*, 19(8), 2935–2948. <https://doi.org/10.1111/1462-2920.13766>

877 Hubbard, S. S., Williams, K. H., Agarwal, D., Banfield, J., Beller, H., Bouskill, N., Brodie, E.,
878 Carroll, R., Dafflon, B., Dwivedi, D., Falco, N., Faybishenko, B., Maxwell, R., Nico, P.,
879 Steefel, C., Steltzer, H., Tokunaga, T., Tran, P. A., Wainwright, H., & Varadharajan, C.
880 (2018). The East River, Colorado, Watershed: A Mountainous Community Testbed for
881 Improving Predictive Understanding of Multiscale Hydrological–Biogeochemical
882 Dynamics. *Vadose Zone Journal*, 17(1), 180061. <https://doi.org/10.2136/vzj2018.03.0061>

883 Huning, L. S., & AghaKouchak, A. (2018). Mountain snowpack response to different levels of
884 warming. *Proceedings of the National Academy of Sciences*, 115(43), 10932–10937.
885 <https://doi.org/10.1073/pnas.1805953115>

886 James, A. L., & Roulet, N. T. (2009). Antecedent moisture conditions and catchment
887 morphology as controls on spatial patterns of runoff generation in small forest catchments.
888 *Journal of Hydrology*, 377(3), 351–366. <https://doi.org/10.1016/j.jhydrol.2009.08.039>

889 Jenkins, A., Ferrier, R. C., Harriman, R., & Ogunkoya, Y. O. (1994). A case study in catchment
890 hydrochemistry: Conflicting interpretations from hydrological and chemical observations.
891 *Hydrological Processes*, 8(4), 335–349. <https://doi.org/10.1002/hyp.3360080406>

892 Kiewiet, L., Meerveld, I. van, & Seibert, J. (2020). Effects of Spatial Variability in the
893 Groundwater Isotopic Composition on Hydrograph Separation Results for a Pre-Alpine
894 Headwater Catchment. *Water Resources Research*, 56(7), e2019WR026855.
895 <https://doi.org/10.1029/2019WR026855>

896 Klaus, J., & McDonnell, J. J. (2013). Hydrograph separation using stable isotopes: Review and
897 evaluation. *Journal of Hydrology*, 505, 47–64.
898 <https://doi.org/10.1016/j.jhydrol.2013.09.006>

899 Knowles, N., Dettinger, M. D., & Cayan, D. R. (2006). Trends in Snowfall versus Rainfall in the
900 Western United States. *Journal of Climate*, 19(18), 4545–4559.
901 <https://doi.org/10.1175/JCLI3850.1>

902 Kopytkovskiy, M., Geza, M., & McCray, J. E. (2015). Climate-change impacts on water
903 resources and hydropower potential in the Upper Colorado River Basin. *Journal of*
904 *Hydrology: Regional Studies*, 3, 473–493. <https://doi.org/10.1016/j.ejrh.2015.02.014>

905 Ladouche, B., Probst, A., Viville, D., Idir, S., Baqué, D., Loubet, M., Probst, J.-L., & Bariac, T.
906 (2001). Hydrograph separation using isotopic, chemical and hydrological approaches
907 (Strengbach catchment, France). *Journal of Hydrology*, 2(3–4), 255–274.

908 Lawrence, C. R., Painter, T. H., Landry, C. C., & Neff, J. C. (2010). Contemporary geochemical
909 composition and flux of aeolian dust to the San Juan Mountains, Colorado, United States.
910 *Journal of Geophysical Research: Biogeosciences*, 115(G3).
911 <https://doi.org/10.1029/2009JG001077>

912 Li, D., Wrzesien, M. L., Durand, M., Adam, J., & Lettenmaier, D. P. (2017). How much runoff
913 originates as snow in the western United States, and how will that change in the future?

914 *Geophysical Research Letters*, 44(12), 6163–6172.
915 <https://doi.org/10.1002/2017GL073551>

916 Liu, F., Conklin, M. H., & Shaw, G. D. (2017). Insights into hydrologic and hydrochemical
917 processes based on concentration–discharge and end-member mixing analyses in the mid-
918 Merced River Basin, Sierra Nevada, California. *Water Resources Research*, 53(1), 832–
919 850. <https://doi.org/10.1002/2016WR019437>

920 Liu, F., Williams, M. W., & Caine, N. (2004). Source waters and flow paths in an alpine
921 catchment, Colorado Front Range, United States. *Water Resources Research*, 40(9).
922 <https://doi.org/10.1029/2004WR003076>

923 Lukens, Eileen Page, "Evaluation of Hydrograph Separation Techniques with Uncertain End-
924 Member Composition" (2022). *All Graduate Theses and Dissertations*. 8446.
925 <https://digitalcommons.usu.edu/etd/8446>

926 Miller, M. P., Susong, D. D., Shope, C. L., Heilweil, V. M., & Stolp, B. J. (2014). Continuous
927 estimation of baseflow in snowmelt-dominated streams and rivers in the Upper Colorado
928 River Basin: A chemical hydrograph separation approach. *Water Resources Research*,
929 50(8), 6986–6999. <https://doi.org/10.1002/2013WR014939>

930 Mote, P. W., Hamlet, A. F., Clark, M. P., & Lettenmaier, D. P. (2005). Declining Mountain
931 Snowpack in Western North America. *Bulletin of the American Meteorological Society*,
932 86(1), 39–50. <https://doi.org/10.1175/BAMS-86-1-39>

933 Mote, P. W., Li, S., Lettenmaier, D. P., Xiao, M., & Engel, R. (2018). Dramatic declines in
934 snowpack in the western US. *Npj Climate and Atmospheric Science*, 1(1), 1–6.
935 <https://doi.org/10.1038/s41612-018-0012-1>

936 Painter, T. H., Barrett, A. P., Landry, C. C., Neff, J. C., Cassidy, M. P., Lawrence, C. R.,
937 McBride, K. E., & Farmer, G. L. (2007). Impact of disturbed desert soils on duration of
938 mountain snow cover. *Geophysical Research Letters*, 34(12).
939 <https://doi.org/10.1029/2007GL030284>

940 Painter, T. H., Deems, J. S., Belnap, J., Hamlet, A. F., Landry, C. C., & Udall, B. (2010).
941 Response of Colorado River runoff to dust radiative forcing in snow. *Proceedings of the*
942 *National Academy of Sciences*, 107(40), 17125–17130.
943 <https://doi.org/10.1073/pnas.0913139107>

944 Penna, D., & Meerveld, H. J. (Ilja) van. (2019). Spatial variability in the isotopic composition of
945 water in small catchments and its effect on hydrograph separation. *WIREs Water*, 6(5),
946 e1367. <https://doi.org/10.1002/wat2.1367>

947 Pinder, G. F., & Jones, J. F. (1969). Determination of the ground-water component of peak
948 discharge from the chemistry of total runoff. *Water Resources Research*, 5(2), 438–445.
949 <https://doi.org/10.1029/WR005i002p00438>

950 PRISM Climate Group, Oregon State University, <http://prism.oregonstate.edu>, created 4 Feb
951 2021

952 Qin, Y., Abatzoglou, J. T., Siebert, S., Huning, L. S., AghaKouchak, A., Mankin, J. S., Hong, C.,
953 Tong, D., Davis, S. J., & Mueller, N. D. (2020). Agricultural risks from changing
954 snowmelt. *Nature Climate Change*, 10(5), 459–465. <https://doi.org/10.1038/s41558-020-0746-8>

955

956 Skiles, S. M., Painter, T. H., Belnap, J., Holland, L., Reynolds, R. L., Goldstein, H. L., & Lin, J.
957 (2015). Regional variability in dust-on-snow processes and impacts in the Upper Colorado
958 River Basin. *Hydrological Processes*, 29(26), 5397–5413.
959 <https://doi.org/10.1002/hyp.10569>

- 960 Skiles, S. M., Painter, T. H., Deems, J. S., Bryant, A. C., & Landry, C. C. (2012). Dust radiative
961 forcing in snow of the Upper Colorado River Basin: 2. Interannual variability in radiative
962 forcing and snowmelt rates. *Water Resources Research*, *48*(7).
963 <https://doi.org/10.1029/2012WR011986>
- 964 Sklash, M. G., & Farvolden, R. N. (1979). The role of groundwater in storm runoff. *Journal of*
965 *Hydrology*, *43*(1), 45–65. [https://doi.org/10.1016/0022-1694\(79\)90164-1](https://doi.org/10.1016/0022-1694(79)90164-1)
- 966 Stewart, I. T., Cayan, D. R., & Dettinger, M. D. (2005). Changes toward Earlier Streamflow
967 Timing across Western North America. *Journal of Climate*, *18*(8), 1136–1155.
968 <https://doi.org/10.1175/JCLI3321.1>
- 969 Sueker, J. K., Ryan, J. N., Kendall, C., & Jarrett, R. D. (2000). Determination of hydrologic
970 pathways during snowmelt for alpine/subalpine basins, Rocky Mountain National Park,
971 Colorado. *Water Resources Research*, *36*(1), 63–75.
972 <https://doi.org/10.1029/1999WR900296>
- 973 Wels, C., Cornett, R. J., & Lazerte, B. D. (1991). Hydrograph separation: A comparison of
974 geochemical and isotopic tracers. *Journal of Hydrology*, *122*(1), 253–274.
975 [https://doi.org/10.1016/0022-1694\(91\)90181-G](https://doi.org/10.1016/0022-1694(91)90181-G)
- 976 Williams, M. W., Seibold, C., & Chowanski, K. (2009). Storage and release of solutes from a
977 subalpine seasonal snowpack: Soil and stream water response, Niwot Ridge, Colorado.
978 *Biogeochemistry*, *95*(1), 77–94. <https://doi.org/10.1007/s10533-009-9288-x>

TABLES

Table 1: Criteria for evaluating C-Qplots. Criteria are relative to the water year. $slope_{max}$ and R^2_{max} are the maximums found in a single water year. $RMSE_{min}$ was the minimum for the water year.

Rating	Slope	R²	RMSE
Best	$\geq 0.7 slope_{max} $	$\geq 0.8 R^2_{max}$	$\leq 1.2 RMSE_{min}$
Moderate	$\geq 0.5 slope_{max} $	$\geq 0.7 R^2_{max}$	$\leq 1.5 RMSE_{min}$
Poor	$< 0.5 slope_{max} $	$< 0.7 R^2_{max}$	$> 1.5 RMSE_{min}$

Table 2: The mean relative root mean square error (RRMSE) and R^2 for the residuals for each water year. Average values for retaining two to three principal components ($m = 2$ and $m = 3$) fit ranges defined by Table S2. Expanded tables which include p values by solutes are available (Tables S3 – S5)

m	2016 WY		2017 WY		2018 WY	
	RRMSE (%)	R^2	RRMSE (%)	R^2	RRMSE (%)	R^2
1	5.6	0.109	9.6	0.233	8.1	0.141
2	4.1	0.057	4.9	0.055	4.8	0.054
3	2.5	0.024	1.8	0.007	1.4	0.010
4	1.1	0.006				

Table 3: Median fraction of annual end-member contributions to volume water leaving basin the statistically-based (STAT), mass-based (MB) and end-member (EM) characterizations: measured (M) or hydrologically rationalized (H).

WY	End-Member Characterization	Snowmelt (%)		Groundwater (%)	
		STAT	MB	STAT	MB
2016	3 H-EM	58		27	
	2 H-EM	66	65	34	35
	2 M-EM	75	65	25	35
2017	3 H-EM	67		21	
	2 H-EM	73	75	27	25
	2 M-EM	78	72	22	28
2018	3 H-EM	58		35	
	2 H-EM	59	59	41	41
	2 M-EM	74	69	26	31

FIGURE LEGENDS

Figure 1: Study area of the East River Basin Located in the Elk Mountains of Central Colorado. Service Layer Credits: Esri, HERE, Garmin, ©OpenStreetMap contributors, and the GIS user Community.

Figure 2: Experimental design matrix for all three water years. In general, solutes were selected for use in the analysis, then an end-member characterization method was chosen. Next, the hydrograph was separated using one of two techniques. Finally, two or three end-members were used to complete the separation. This led to five unique separations being performed, as indicated by the light grey arrows.

Figure 3: Residuals analysis for the 2016 WY for the solute strontium. Plots on the left show residuals at different numbers (m) of principal component retention and the associated R^2 , RRMSE. p -values indicate if slope is significantly ($p < 0.05$) different than zero. Open dots represent data points; line evaluates trends in data. Right hand plots assess normality at each level of principal component retention. Plus signs represent the residuals, dashed line represents the theoretical normal distribution residuals would follow if they were normally distributed.

Figure 4: Data projected into the U -space across all WYs as defined by the principal components (PCs). All years include projections using Ba, Mg, Sr, and U. The 2016 WY additionally includes Mg. Error bars represent one standard deviation of the end-member concentrations about the mean from the field data, not the generated distributions of end-member concentrations used for hydrograph separation. Solute are in grey. Hydrologically rationalized end-members (H-EM) concentrations are represented by triangles. Measured end-member (M-EM) concentrations are represented by squares.

Figure 5: Hydrograph separation of three end-members with hydrologically rationalized concentrations (3 H-EM) using the statistically-based method of separation. Lines indicate median response from 1000 samplings around the mean and standard deviation of the end-member concentrations. The interquartile range (IQR) of the model traces shaded around the median represents the lower 25th to upper 75th quantiles.

Figure 6: Hydrograph separation of two end-members with measured concentrations (2 M-EM) using the statistically-based method of separation. Lines indicate median response to 1000 samplings of the end-member concentration distributions. The interquartile range (IQR) of the model traces shaded around the median represents the lower 25th to upper 75th quantiles.

Figure 7: Plots on the left show predicted versus measured concentrations of the instream using 2 end-members characterized by measured concentrations in the 2016 WY. Trends indicated by red line. Dashed lined shows the theoretical perfect prediction of instream concentrations. Middle plots show residuals between predicted and measured instream concentration data. Histogram on the right show the distribution of residuals.

Figure 8: Plots on the left show predicted versus measured concentrations of the instream using two end-members characterized by hydrologic rationalization in the 2016 WY. Trends indicated by red line. Dashed lined shows the theoretical perfect prediction of instream concentrations. Middle plots show residuals between predicted and measured instream concentration data. Histogram on the right show the distribution of residuals.

Figure 9: Hydrograph separation of two end-members with hydrologically rationalized concentrations (2 H-EM) using the mass-based method of separation. Lines indicate median response from four solutes (Ba, Ca, Sr, U) where each end-member concentration for each solute was sampled 1000 times. The

interquartile range (IQR) of the model traces shaded around the median represents the lower 25th to upper 75th quantiles.

Figure 10: Hydrograph separation of two end-members with measured concentrations (2 M-EM) using the mass-based method of separation. Lines indicate median response from all solutes except calcium where each end-member concentration for each solute was sampled 1000 times. The interquartile range (IQR) of the model traces shaded around the median represents the lower 25th to upper 75th quantiles.

Figure 11: Total percent of the annual volume of water leaving the catchment coming from each end-member – groundwater (GW) or snowmelt (snow)- via statistically-based (STAT) and mass-based (MB) methods of separation with hydrologically rationalized end-members concentration (H-EM) and measured end-member concentrations (M-EM). Targets represent the median, boxes represent the interquartile range (IQR) spanning the 25th to 75th quantiles with error bars representing the minimum and maximum, and boxes representing outliers (1.5IQR). The snow end-member is represented in orange, groundwater in blue. H-EMs show n = 1000 for all years while M-EMs show n = 4000 (n = 5000 for 2016WY only)

SUPPLEMENTAL INFORMATION

Supporting information contains more detailed methods for the principal component analysis. Additionally, it contains figures and tables to support the main text, particularly with regards to the residuals analysis and hydrograph separations.

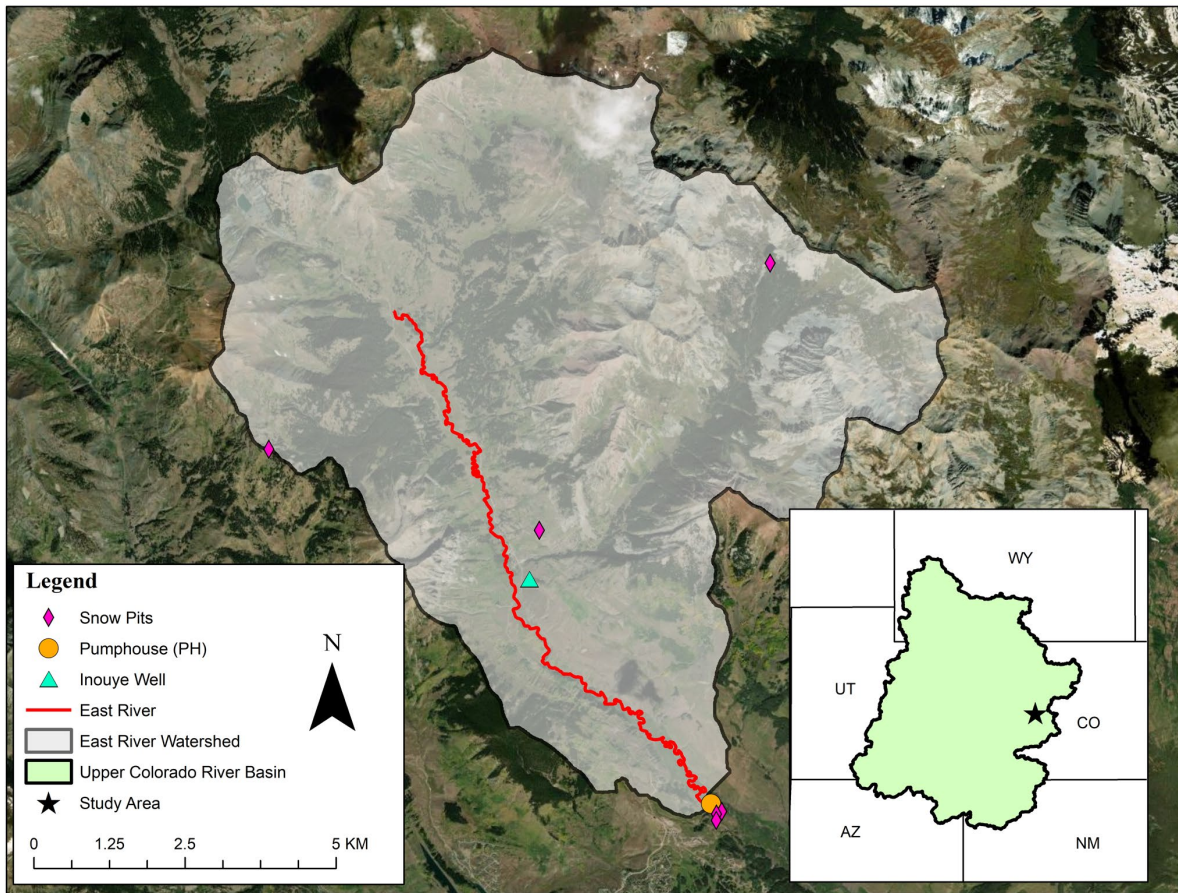


Figure 1: Study area of the East River Basin Located in the Elk Mountains of Central Colorado. Service Layer Credits: Esri, HERE, Garmin, ©OpenStreetMap contributors, and the GIS user Community.

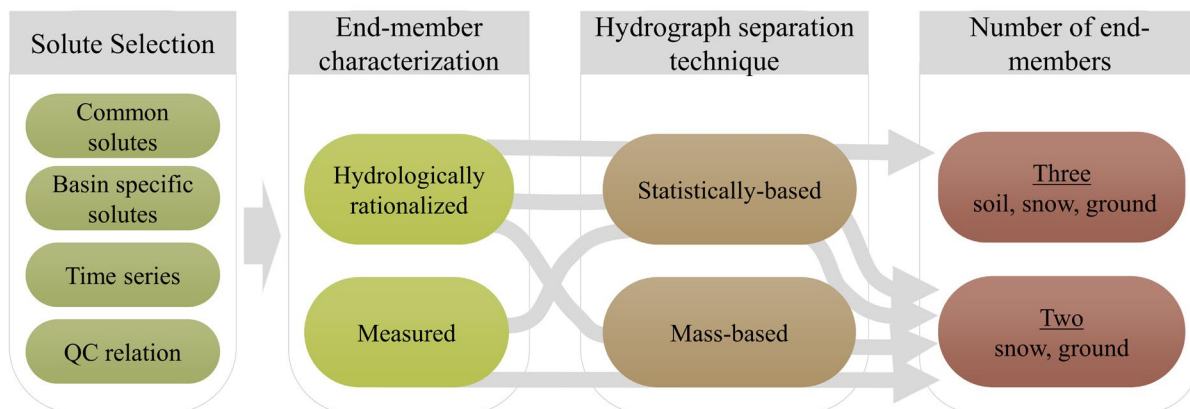


Figure 2: Experimental design matrix for all three water years. In general, solutes were selected for use in the analysis, then an end-member characterization method was chosen. Next, the hydrograph was separated using one of two techniques. Finally, two or three end-members were used to complete the separation. This led to five unique separations being performed, as indicated by the light grey arrows.

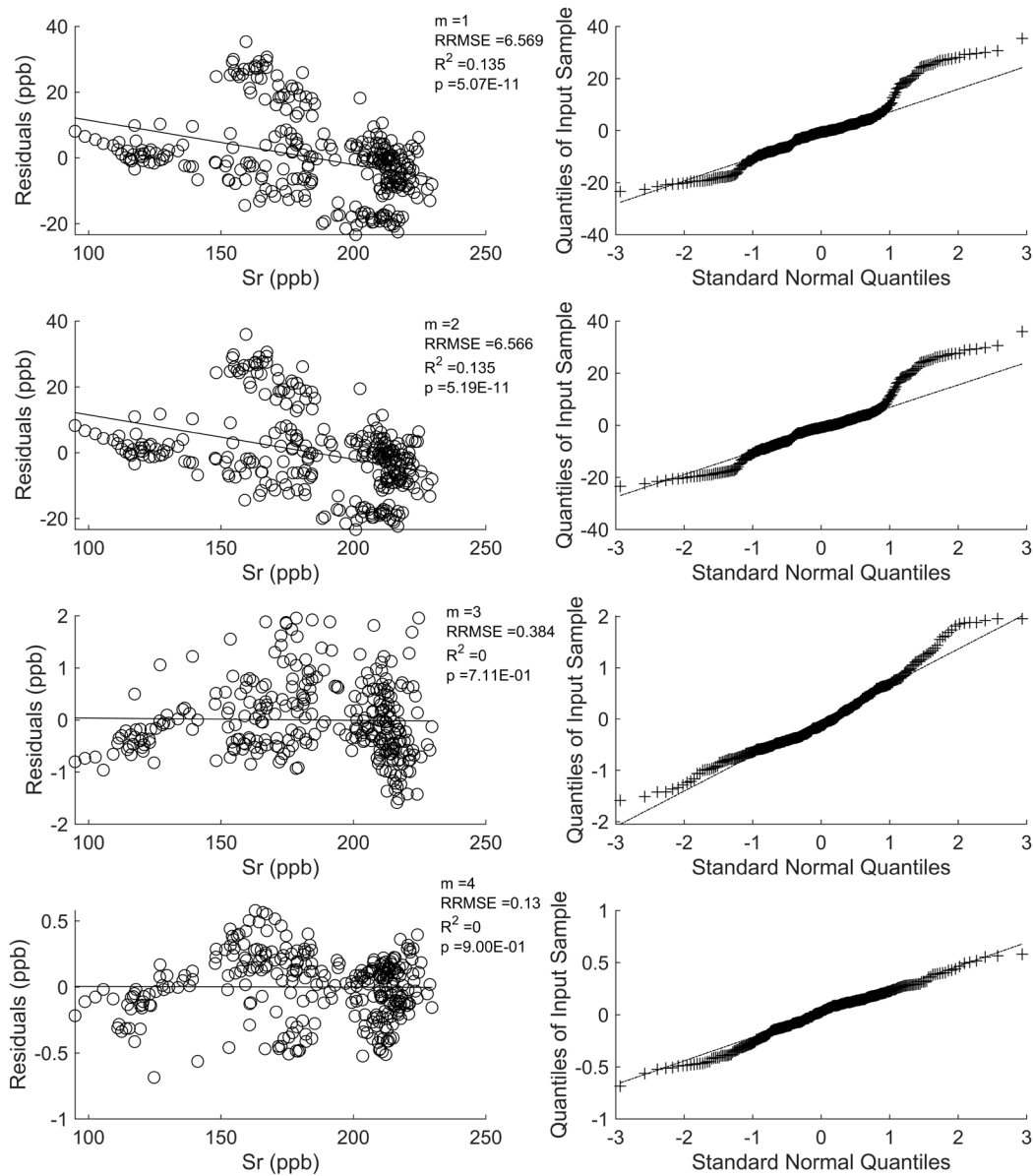


Figure 3: Residuals analysis for the 2016 WY for the solute strontium. Plots on the left show residuals at different numbers (m) of principal component retention and the associated R², RRMSE. p-values indicate if slope is significantly ($p < 0.05$) different than zero. Open dots represent data points; line evaluates trends in data. Right hand plots assess normality at each level of principal component retention. Plus signs represent the residuals, dashed line represents the theoretical normal distribution residuals would follow if they were normally distributed.

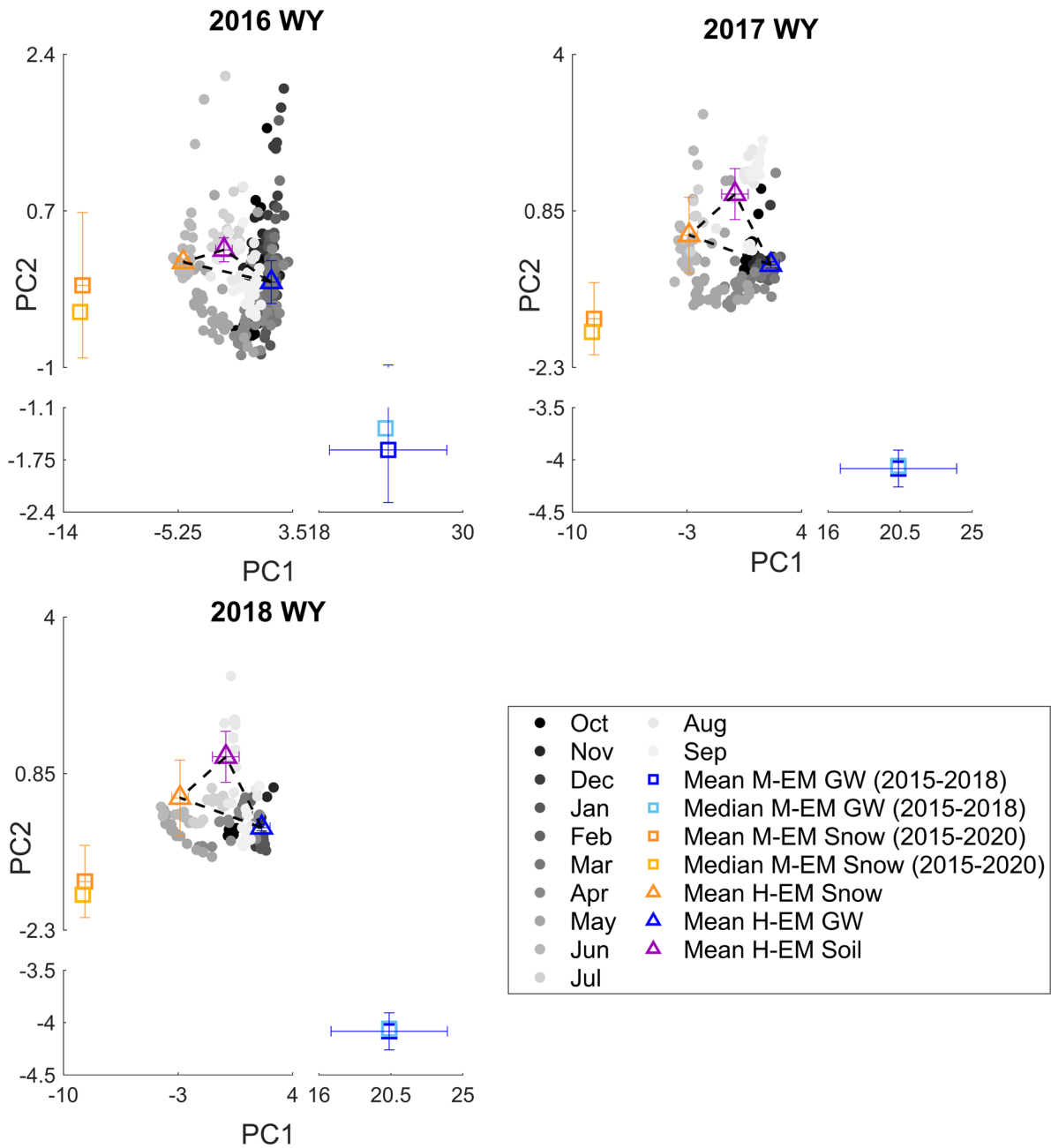


Figure 4: Data projected into the U -space across all WYs as defined by the principal components (PCs). All years include projections using Ba, Mg, Sr, and U. The 2016 WY additionally includes Mg. Error bars represent one standard deviation of the end-member concentrations about the mean from the field data, not the generated distributions of end-member concentrations used for hydrograph separation. Solutes are in grey. Hydrologically rationalized end-members (H-EM) concentrations are represented by triangles. Measured end-member (M-EM) concentrations are represented by squares.

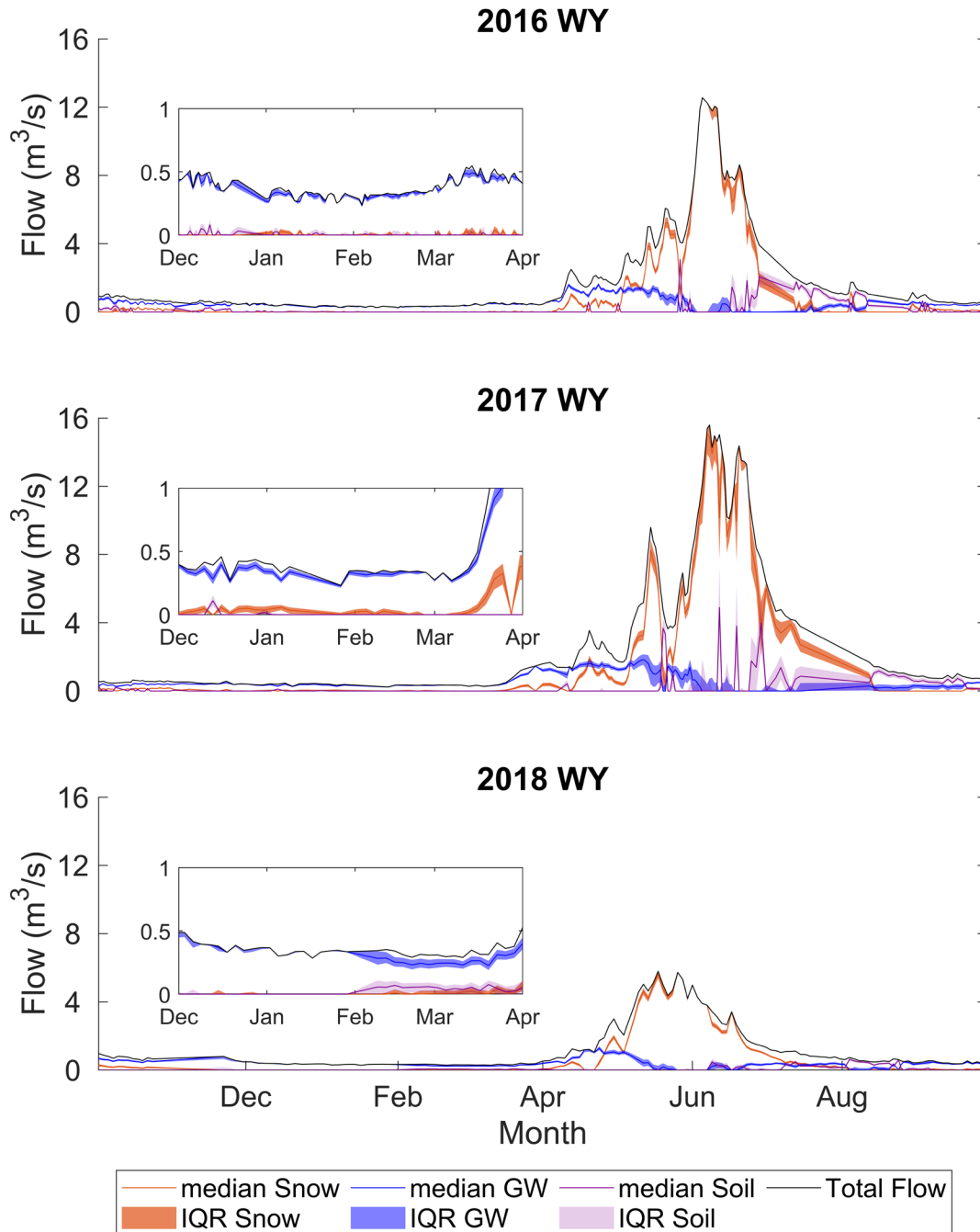


Figure 5: Hydrograph separation of three end-members with hydrologically rationalized concentrations (3 H-EM) using the statistically-based method of separation. Lines indicate median response from 1000 samplings around the mean and standard deviation of the end-member concentrations. The interquartile range (IQR) of the model traces shaded around the median represents the lower 25th to upper 75th quantiles.

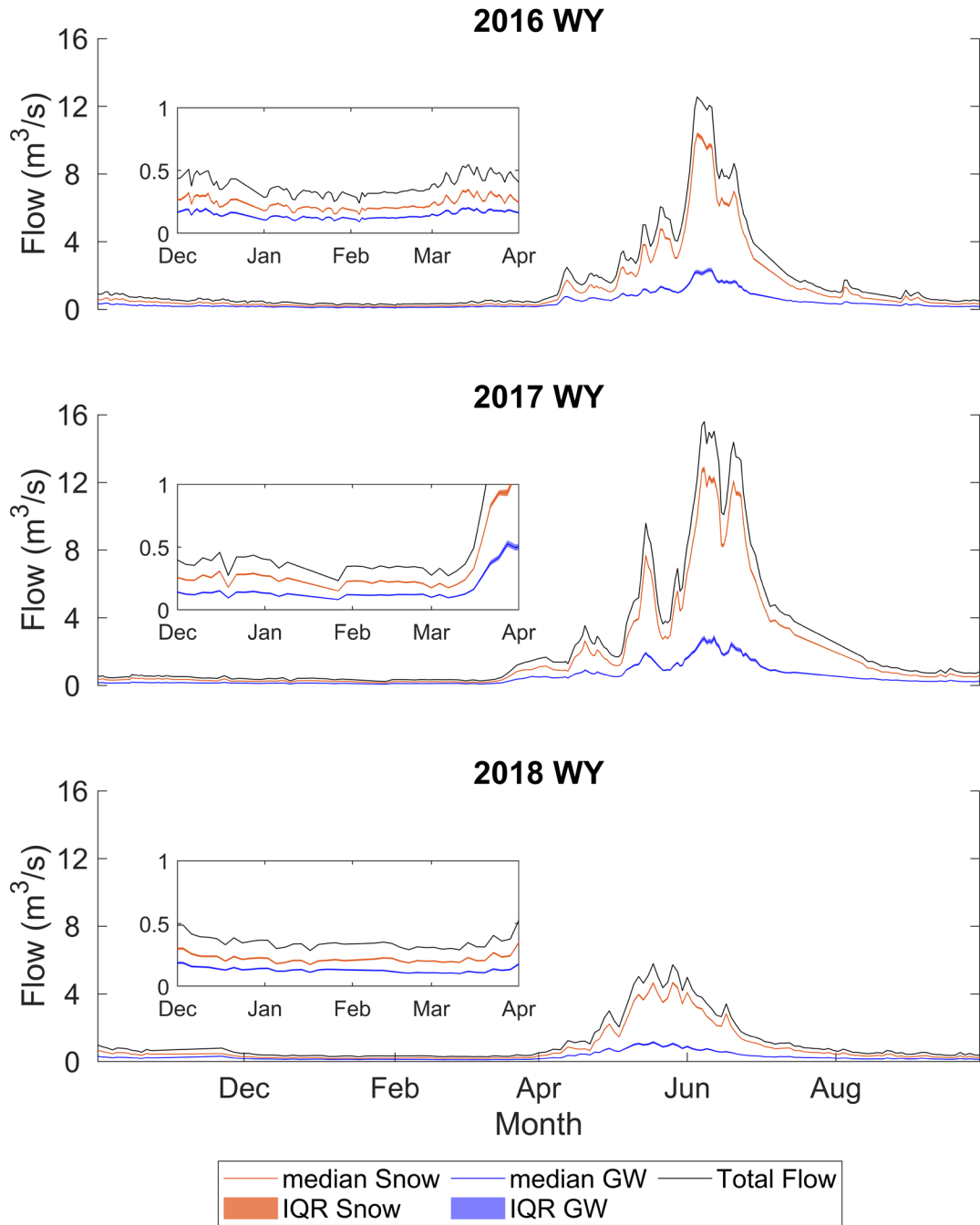


Figure 6: Hydrograph separation of two end-members with measured concentrations (2 M-EM) using the statistically-based method of separation. Lines indicate median response to 1000 samplings of the end-member concentration distributions. The interquartile range (IQR) of the model traces shaded around the median represents the lower 25th to upper 75th quantiles.

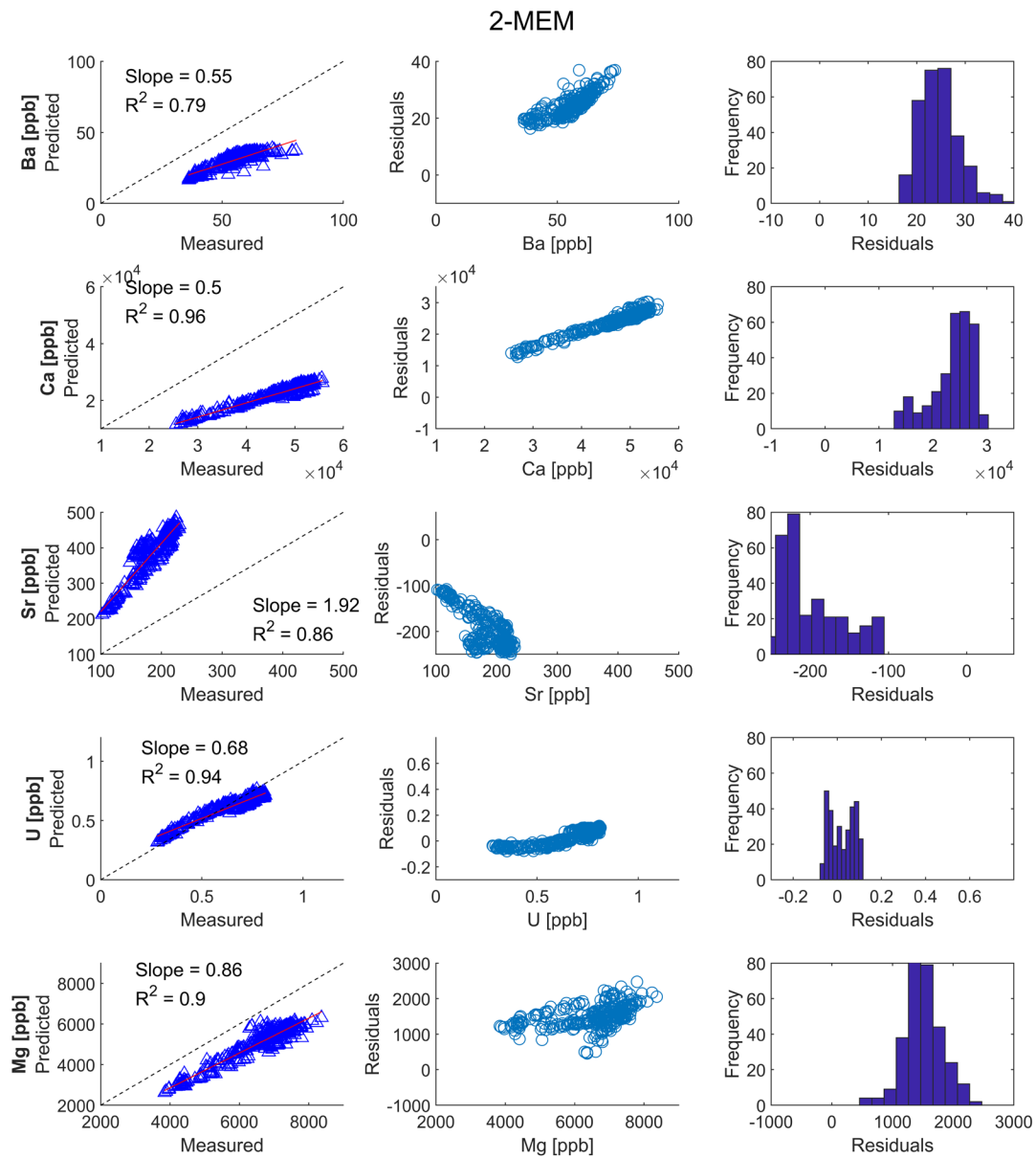


Figure 7: Plots on the left show predicted versus measured concentrations of the instream using 2 end-members characterized by measured concentrations in the 2016 WY. Trends indicated by red line. Dashed lined shows the theoretical perfect prediction of instream concentrations. Middle plots show residuals between predicted and measured instream concentration data. Histogram on the right show the distribution of residuals.

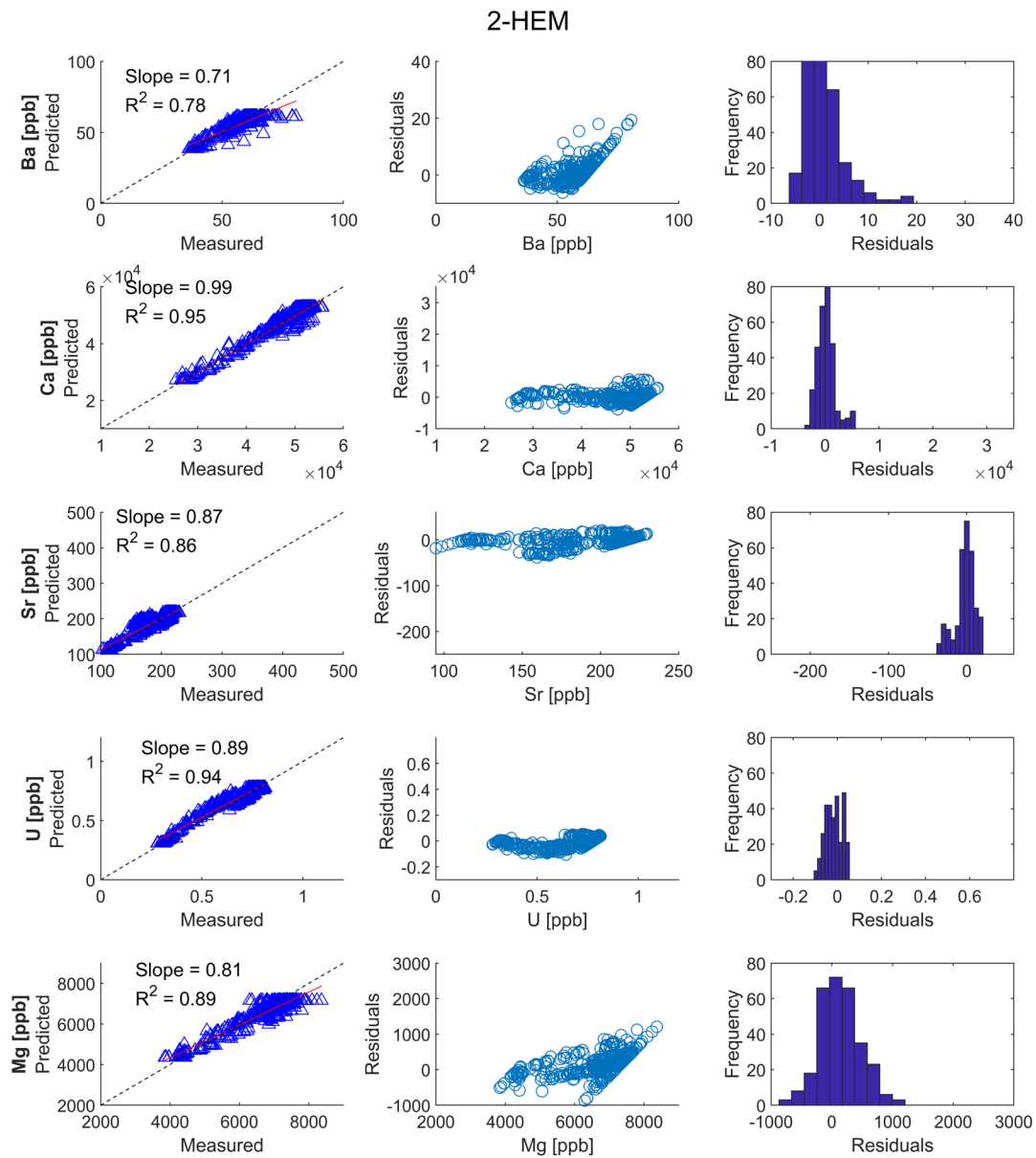


Figure 8: Plots on the left show predicted versus measured concentrations of the instream using two end-members characterized by hydrologic rationalization in the 2016 WY. Trends indicated by red line. Dashed lined shows the theoretical perfect prediction of instream concentrations. Middle plots show residuals between predicted and measured instream concentration data. Histogram on the right show the distribution of residuals.

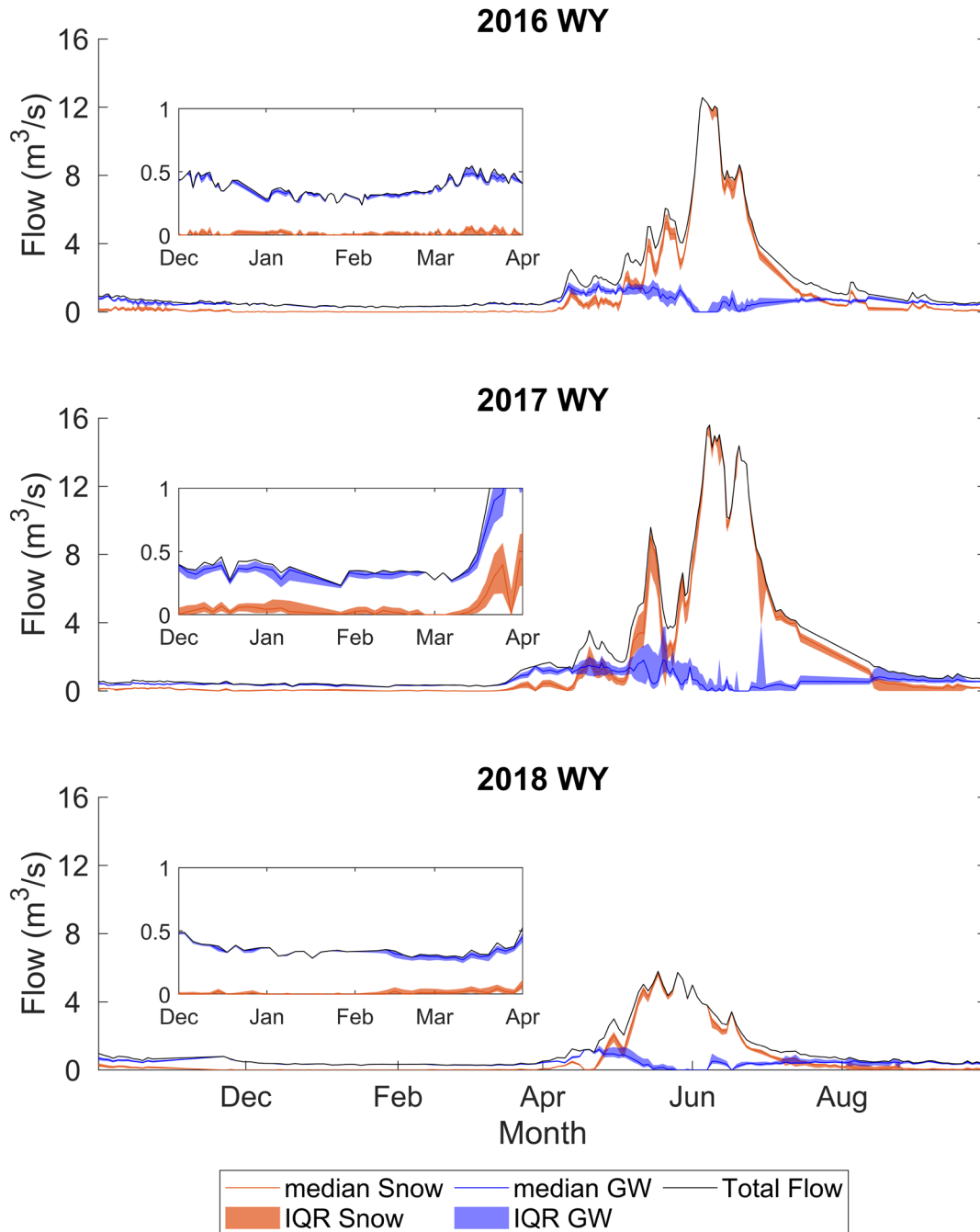


Figure 9: Hydrograph separation of two end-members with hydrologically rationalized concentrations (2 H-EM) using the mass-based method of separation. Lines indicate median response from four solutes (Ba, Ca, Sr, U) where each end-member concentration for each solute was sampled 1000 times. The interquartile range (IQR) of the model traces shaded around the median represents the lower 25th to upper 75th quantiles.

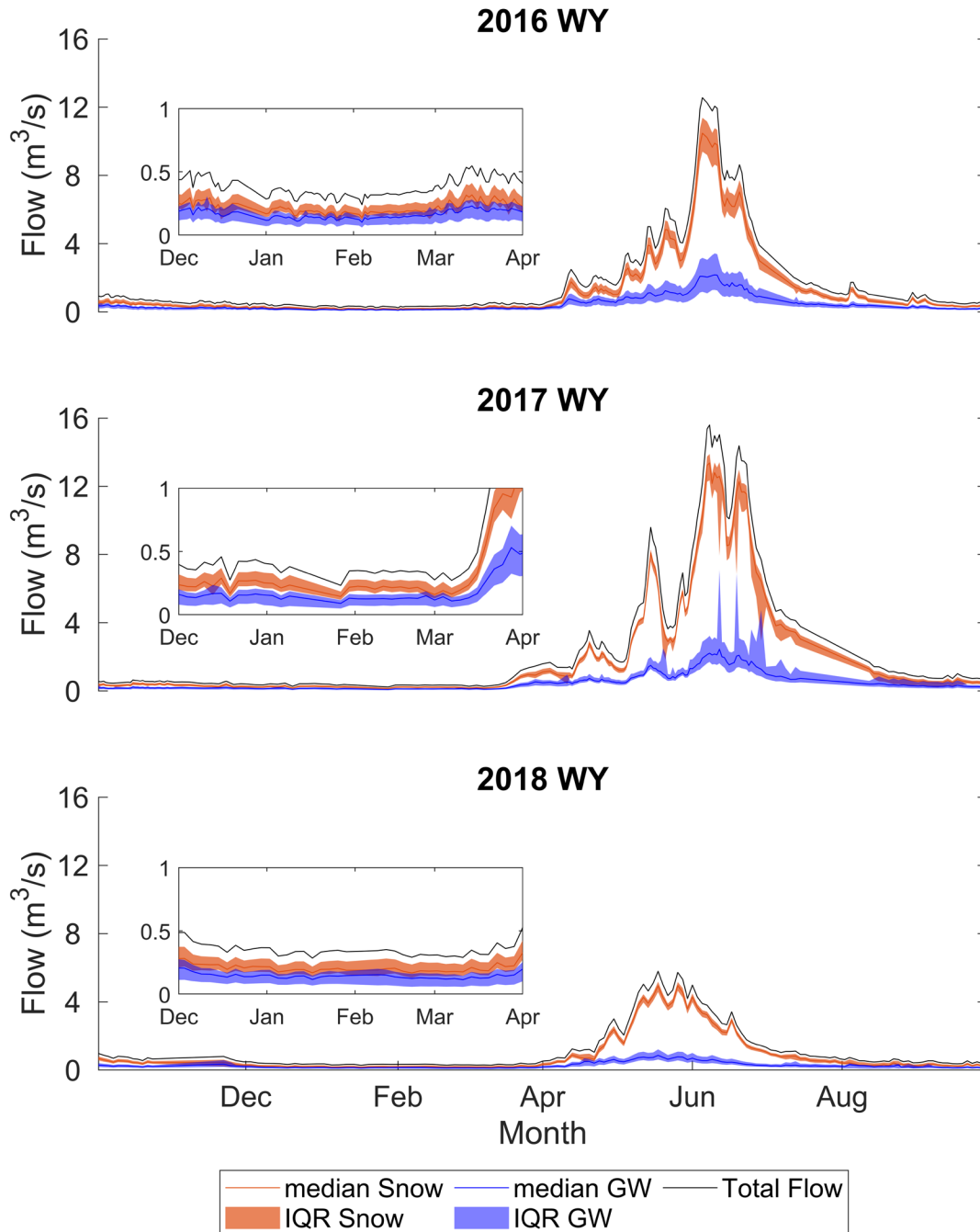


Figure 10: Hydrograph separation of two end-members with measured concentrations (2 M-EM) using the mass-based method of separation. Lines indicate median response from all solutes except calcium where each end-member concentration for each solute was sampled 1000 times. The interquartile range (IQR) of the model traces shaded around the median represents the lower 25th to upper 75th quantiles.

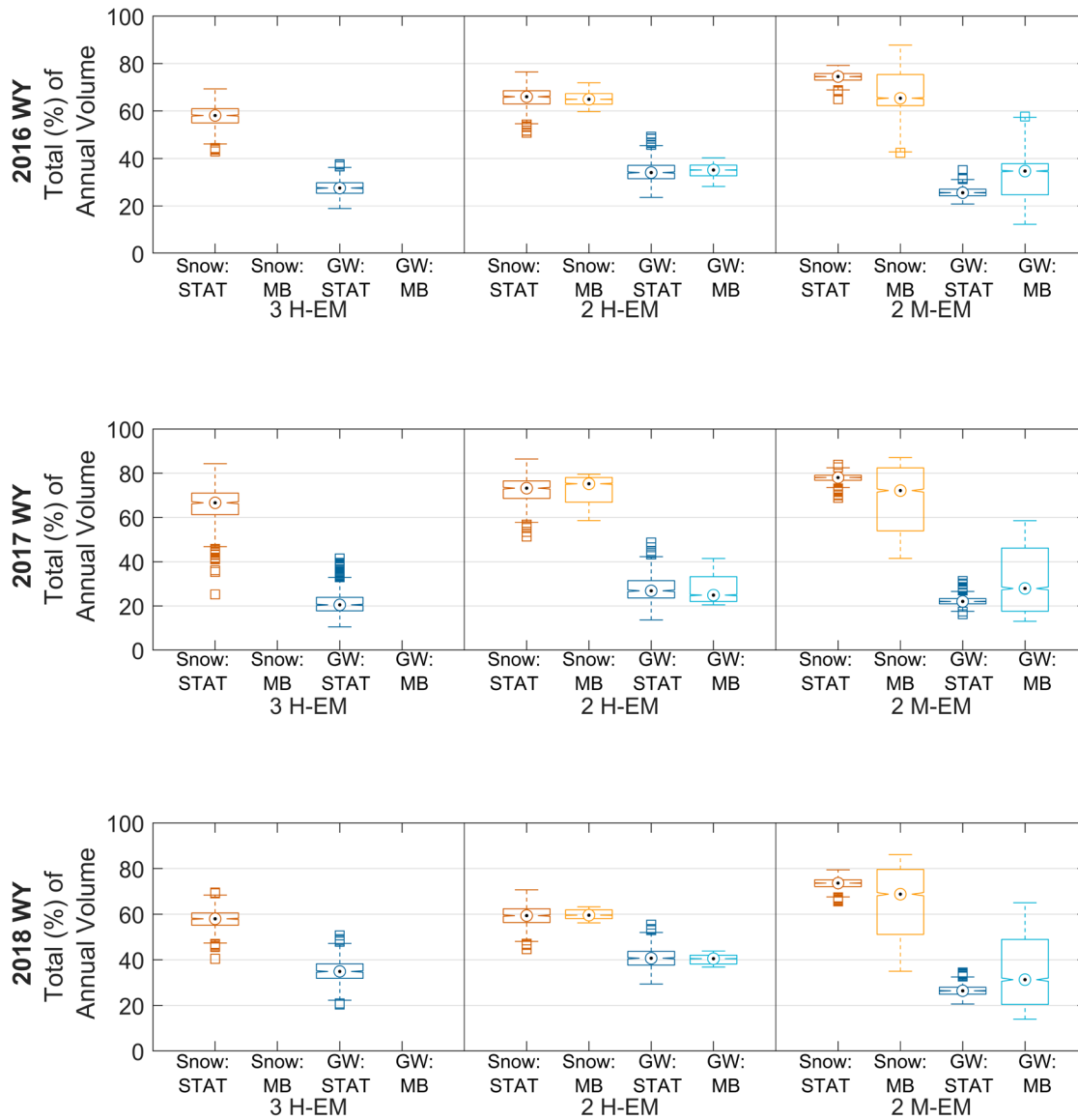


Figure 11: Total percent of the annual volume of water leaving the catchment coming from each end-member – groundwater (GW) or snowmelt (snow)- via statistically-based (STAT) and mass-based (MB) methods of separation with hydrologically rationalized end-members concentration (H-EM) and measured end-member concentrations (M-EM). Targets represent the median, boxes represent the interquartile range (IQR) spanning the 25th to 75th quantiles with error bars representing the minimum and maximum, and boxes representing outliers (1.5IQR). The snow end-member is represented in orange, groundwater in blue. H-EMs show n = 1000 for all years while M-EMs show n = 4000 (n = 5000 for 2016WY only)

